Bulletin of the Czech Geological Survey, Vol. 77, No. 2, 67–92, 2002

From explosive breccia to unidirectional solidification textures: magmatic evolution of a phosphorus- and fluorine-rich granite system (Podlesí, Krušné hory Mts., Czech Republic)

KAREL BREITER

Czech Geological Survey, Geologická 6, 152 00 Praha 5, Czech Republic; e-mail: breiter@cgu.cz

Abstract. The Podlesí granite stock in western Krušné hory Mts. represents the most highly fractionated part of the late Variscan Nejdek-Eibenstock pluton. Internal fabric of the stock has been studied in several boreholes up to 350 m deep. The stock is composed of two tongue-like bodies of albite-protolithionite-topaz granite (stock granite) coalesced at depth, which were emplaced into Ordovician phyllite and biotite granite of younger intrusive complex (YIC) of the Nejdek pluton. The uppermost part of the intrusion is bordered by a layer of marginal pegmatite (stockscheider) up to 50 cm thick. Explosive breccia was found as an isolated block at the southwest contact of the stock. It is comprised of fragments of phyllite several millimetres to 5 cm in size cemented with fine-grained granitic matrix similar to the stock granite, but very fine-grained.

Within the uppermost 100 m, the stock granite is intercalated with several mostly flat-lying dykes of albite-zinnwaldite-topaz granite (dyke granite). Upper and lower contacts of the dykes are sharp, flat, but in detail slightly uneven. The thickest dyke (about 7 m) outcrops in an old quarry. A prominent example of layering with unidirectional solidification textures (UST) was found in the upper part of this major dyke. Individual Q-Afs laminae are separated by comb quartz layers and/or by layers of oriented fan-like zinnwaldite aggregates. A pegmatite-like layer with oriented megacrysts of Kfs up to 6 cm long was encountered in the uppermost part of the dyke. One thin layer of fine-grained quartz with oriented Kfs-megacrysts was found within the stock granite.

Post-magmatic processes, particularly greisenisation, developed only to a limited degree. The uppermost flat dyke of the dyke granite was partly greisenised into white quartz-rich (+topaz, Li-mica, wolframite) greisen. Scarce thin, steep stringers of biotite greisen were encountered over the entire outcrop and in drilled parts of the stock granite and surrounding biotite granite.

The stock granite is strongly peraluminous (A/CNK 1.15–1.25), enriched in incompatible elements such as Li, Rb, Cs, Sn, Nb, W, and poor in Mg, Ca, Sr, Ba, Fe, Sc, Zr, Pb, and V. The rock is rich in phosphorus (0.4–0.8 wt% P_2O_5) and fluorine (0.6–1.8 wt% F). A high degree of magmatic fractionation is demonstrated by low K/Rb and Zr/Hf ratios (22–35 and 12–20, respectively) and high U/Th ratio (4–7). The dyke granite is even more enriched in Al (A/CNK = 1.2–1.4), P (0.6–1.5 wt% P_2O_5), F (1.4–2.4 wt%), Na, Rb, Li, Nb, Ta, and depleted in Si, Zr, Sn, W and REE. The K/Rb (14–20) and Zr/Hf (9–13) ratios are lower than in the stock granite.

Based on all available data, the following evolutionary model was developed: Pronounced fractionation of the YIC-melt (=Younger Intrusive Complex of the Nejdek pluton) produced small amount of residual F, P, Li-rich melt (stock granite melt) which was emplaced at a "shallow depth" as a tongue-like body. The rapid emplacement was accompanied by brecciation of the overlying phyllite. Composition of the emplaced "primary" melt was similar to the present stock granite. Its crystallisation started in the outer upper part of the stock. This represents the rapidly cooled primary melt without major late- and post-magmatic alteration. Beneath the rapidly crystallised carapace, water and volatiles became enriched. Subsequent fractionation in deeper parts of the stock produced a very small amount of residual melt extremely enriched in F, P, Li and water. When cooling of the upper part of the stock allowed opening of brittle structures, the residual melt intruded upwards, forming a set of generally flat dykes. Crystallisation of the major dykes proceeded in closed-system conditions from the bottom upward. Volatiles and exsolved bubbles of water-rich fluid migrated to the uppermost part of the dykes. When the pressure of exsolved water overcame the lithostatic pressure and cohesion of surrounding rocks, the system opened. Propagation of existing cracks or opening of new cracks started. Vapour escaped and the adiabatic decrease in pressure resulted in sudden decrease in temperature. The UST crystallised from the undercooled melt. This process was repeated several times. Nonequilibrium crystallisation in layered rock produced small domains with contrasting chemistry and finally very small amounts of liquids of unusual composition.

Key words: granite, brecciation, layered intrusion, undirectional solidification textures, chemical composition, fluorine, phosphorus, Krušné hory Mts., Bohemian Massif

Introduction

The Podlesí granite stock is the largest outcrop of extremely fractionated phosphorus-rich Li-mica granite within the Nejdek-Eibenstock pluton (western Krušné hory/Erzgebirge Mts., Czech Republic, Germany). The internal structure of this stock is well documented from boreholes up to 350 m deep. Evolutionary stages of the granite system ranged from magmatic explosive breccia through crystallisation of marginal pegmatite, standard granite crystallisation to formation of dykes and magmatic layering with UST. The minimal post-magmatic hydrothermal processes in the Podlesí granite system permitted the study of features related to the above-mentioned magmatic processes in a volatile-rich, extremely fractionated system without post-magmatic alteration. These features make the Podlesí locality one of the most important granite localities within the Bohemian Massif.

The outcrop of Podlesí granite was first reported in the geological map of Saxony (Schalch et al. 1900), but its very special character was distinguished only several years ago. The first modern geological study and borehole program was conducted by the Czech Geological Survey in 1985–86 as part of an extensive prospecting program for Sn-W ores (Lhotský et al. 1988). From 1994, the Podlesí system was intensively studied from the viewpoint of petrology, mineralogy, geochemistry and geophysics (Frýda and Breiter 1995, Breiter and Seltmann 1995, Breiter et

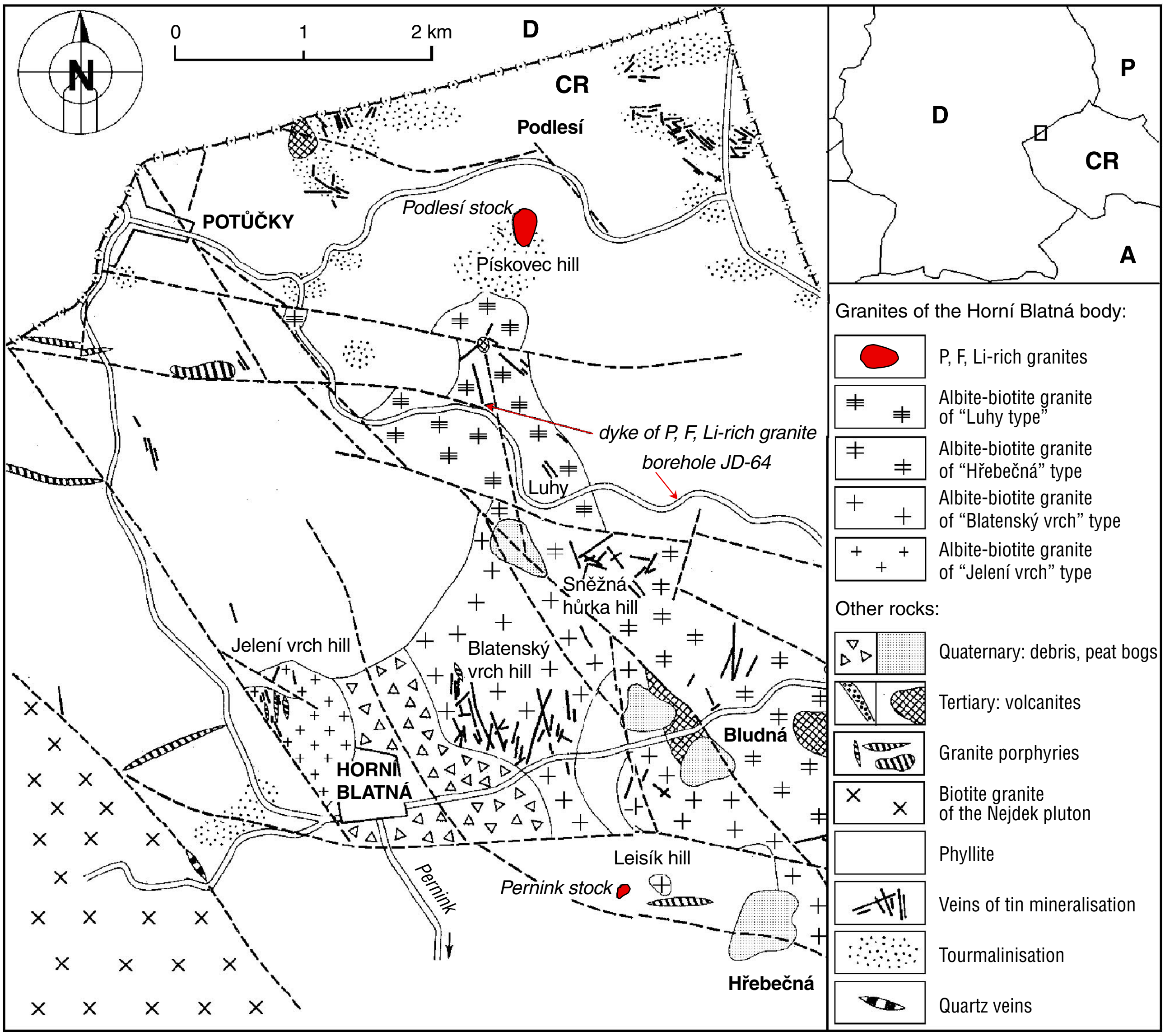

Fig. 1. Geological map of the surrounding of the Podlesí stock.

al. 1997a, b, Breiter 1998, Chlupáčová and Breiter 1998, Táborská and Breiter 1998, Skála et al. 1998, Breiter 2001a).

A new borehole campaign was started by the Czech Geological Survey in autumn 2000. These recent investigations motivated publication of new papers – see the abstract volume of the Podlesí Workshop: Breiter (2001b), Förster (2001), Chlupáčová and Mrázová (2001), Kostitsyn and Breiter (2001), Müller et al. (2001), Žák et al. (2001), and several contributions in this volume.

Geology

The Podlesí granite stock is located in the western part of the Krušné hory/ Erzgebirge Mts. in western Bohemia near the German border. The Podlesí stock represents the most fractionated part of the late Variscan Nejdek-Eibenstock pluton (Figs 1, 2), in the Saxothuringian zone of the Variscan orogen in central Europe. The Podlesí stock was emplaced into Ordovician phyllite and biotite granite of the so-called younger intrusive complex (YIC). The contact of the granite with phyllite and biotite granite is sharp. Phyllite surrounding the granite has been strongly altered to protolithionite-topaz hornfels and is crosscut by aplite dykes, and numerous steep topaz-albite-zinnwaldite-quartz veinlets, accompanied by greisenisation and tourmalinisation of the surrounding rocks. The biotite granite is muscovitised and sericitised for a distance of 5–25 m from the contact.

Internal fabric of the granite stock was studied in several boreholes of the Czech Geological Survey up to 350 m deep (Fig. 3). The overall shape of the intrusion was formerly interpreted as a simple cupola (Breiter et al. 1997a, b, 1998). New boreholes suggest a more complicated shape, composed of two tongue-like bodies that coalesce at depth. The roots of the intrusion appear to extend to the southwest. Several thin dyke-like apophyses (up to 20 cm) of the stock granite were found in phyllitic rocks near the contact.

The Podlesí granite consists mainly of albite-protolithionite-topaz granite (stock granite), which can be divided into two sub-facies: The "upper facies" constitutes the uppermost 30–40 m of the stock; it is fine-grained and porphyritic. This facies forms a carapace of the granite stock and represents rapidly cooled and crystallised parental melt. The "lower facies", which constitutes the main part of the stock, is medium-grained and non-porphyritic. This facies crystallised more slowly from a melt enriched in fluids. The uppermost part of the intrusion is bordered by a layer of marginal pegmatite (stockscheider) up to 50 cm thick.

In the uppermost 100 m, the stock granite is intruded with several generally flat-lying dykes of albite-zinnwaldite-topaz granite (dyke granite). The position of dyke granite is well documented in boreholes and outcrops (Fig. 3). Upper and lower contacts of the dykes are sharp and relatively flat, but in detail slightly uneven. The thickest dyke (about 7 m) outcrops in an old quarry (Fig. 4). A prominent layer with unidirectional solidification textures (USTs) was found in the upper part of this major dyke. Individual quartz-alkalifeldspars (Q-Afs) laminae are separated by comb quartz layers and/or by layers of oriented fan-like zinnwaldite aggregates. A pegmatite-like layer with oriented megacrysts of potassium feldspar (Kfs) up to 6 cm long was encountered in the uppermost part of the dyke. The USTs also consist of segregations of Mn-rich apatite and small pegmatite pods.

One thin layer of fine-grained quartz with oriented megacrysts of K-feldspar was also found in the stock granite above the quarry. Indications of UST should be also found immediately below the stockscheider.

Post-magmatic processes, particularly greisenisation, developed only to a limited degree. Scarce thin and steeply dipping stringers of biotite greisen were encountered over the entire outcrop and in drilled parts of the stock granite and surrounding biotite granite. The uppermost flat dyke of the dyke granite was partly greisenised to white quartz (+topaz, Li-mica, wolframite) – rich greisen.

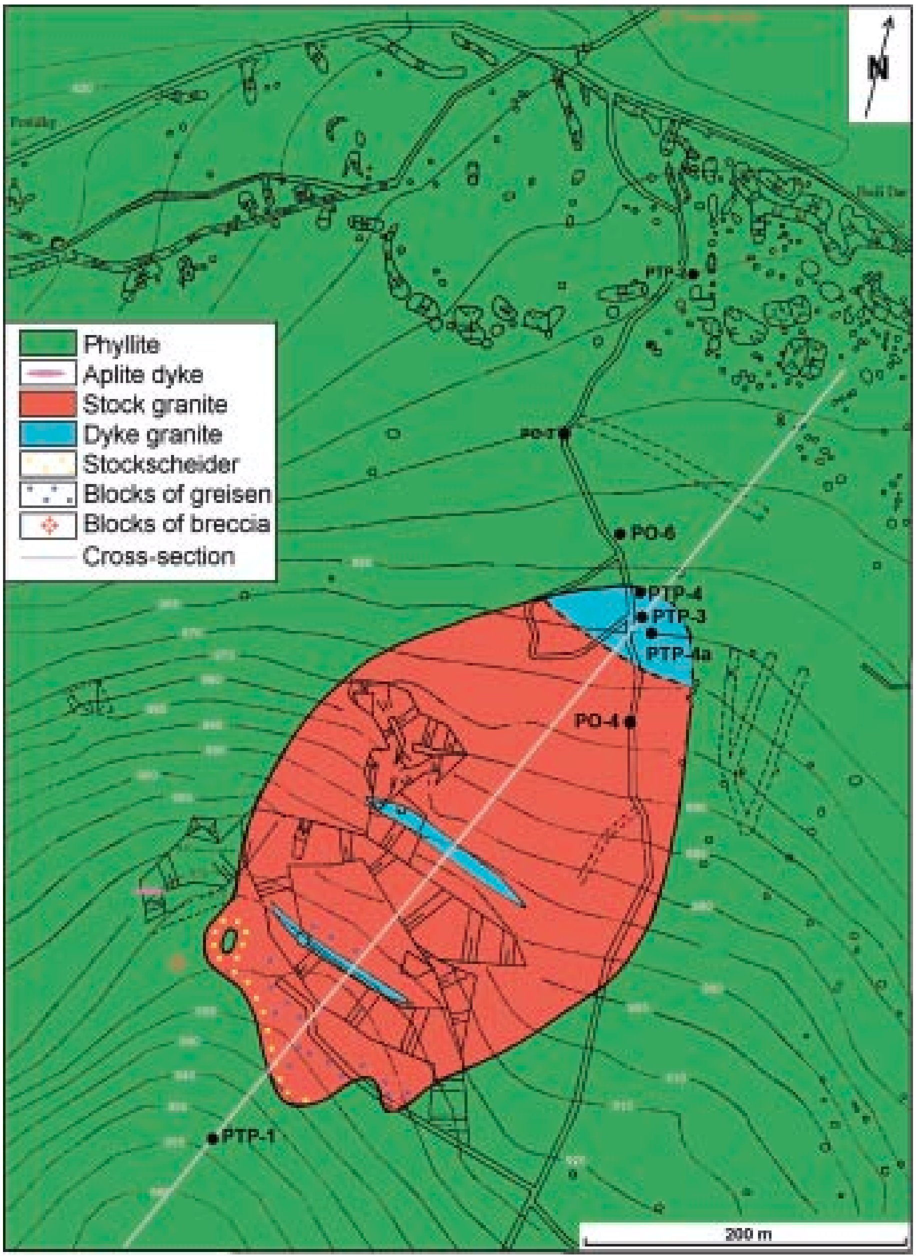

Fig. 2. A detailed geological map of the Podlesí stock.

Petrography

Breccia

Explosive breccia was found only in an isolated block at the SW contact of the stock. It comprises fragments of phyllite several mm to 5 cm in size cemented with fine-grained granitic matrix. Some phyllite fragments are rounded, but others are not (Fig. 5a). Composition of the matrix is similar to that of the stock granite, but very fine-grained. Colum-

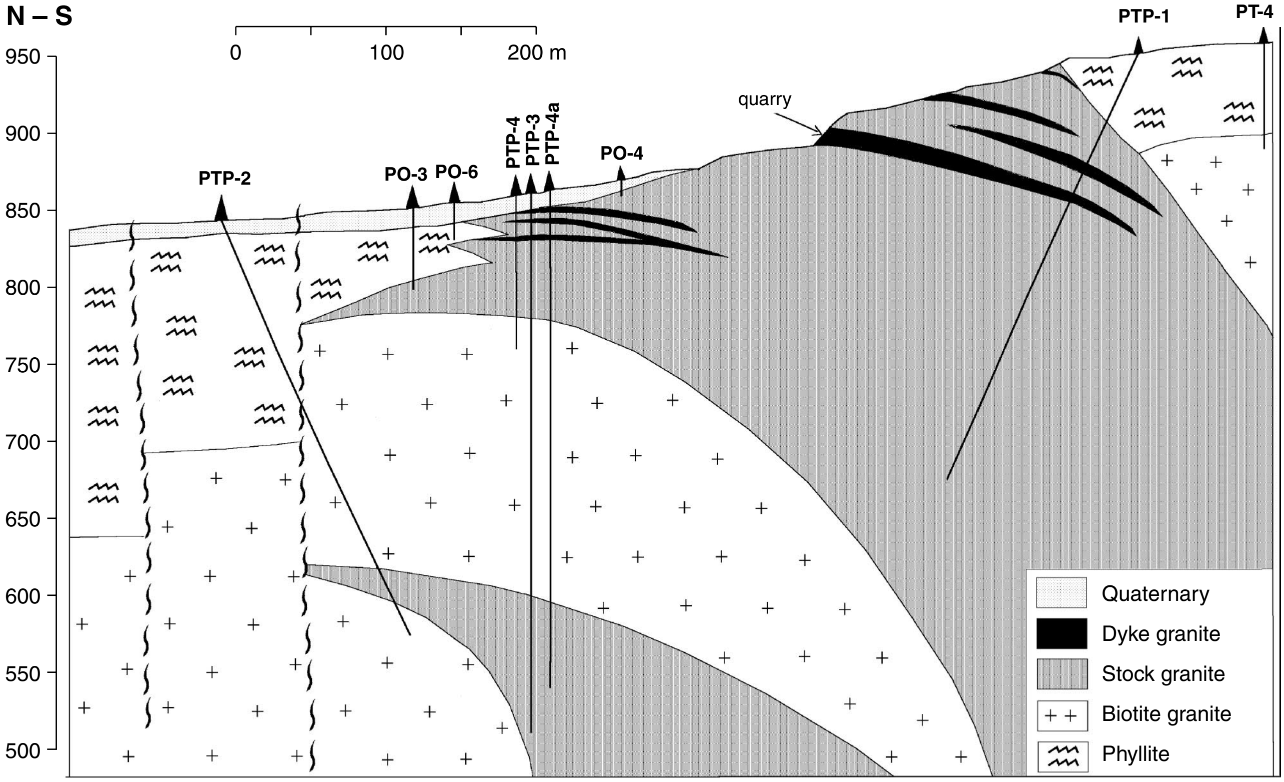

Fig. 3. Geological cross-section.

nar Kfs often grows perpendicular to the phyllite fragments. K-feldspar contains up to 5% of Ab component, plagioclase is pure albite. Both types of feldspars contain up to 0.5 wt% P_2O_5, but the phosphorus distribution is very irregular. Dark mica should be classified as protolithionite. Topaz and apatite are accessory minerals.

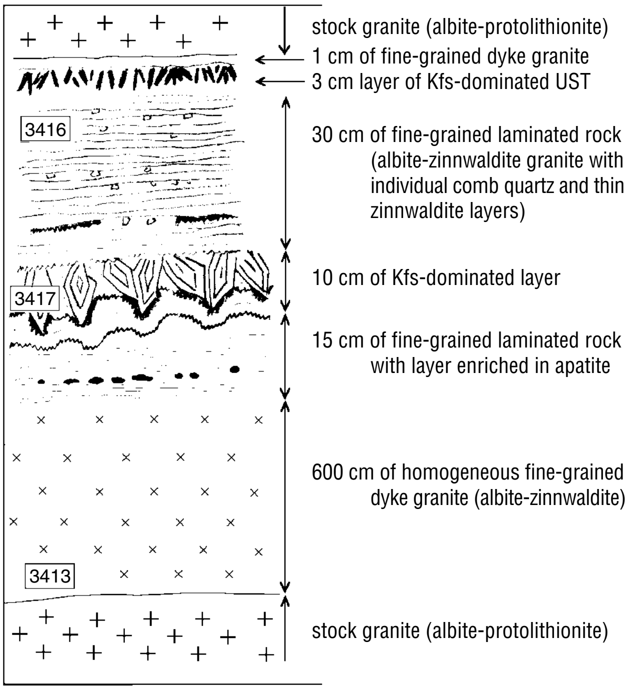

Fig. 4. A sketch of the major dyke.

Stockscheider

Marginal pegmatite or stockscheider is a typical feature of the uppermost parts of tin-bearing granite stocks (Oelsner 1952, Jarchovský 1962). At Podlesí, the stockscheider is developed along the S and SW margin of the body. Generally, it is composed of large prismatic microcline crystals oriented perpendicular to the contact plane of the granite with phyllite. The space between individual microcline crystals is filled with fine-grained granite and, in places, with large grains of milky quartz (Fig. 5b). The granite matrix is enriched in albite, so the bulk composition is similar to that of the stock granite.

The stockscheider zone is 30 to 50 cm thick and grades downward into fine-grained stock granite. In a transitional zone several metres thick, the granite contains individual oriented Kfs crystals up to 10 cm long and 1–2 cm thick (Fig. 5c) and discontinuous layers of comb quartz.

Stock granite

Flesh-coloured albite-protolithionite-topaz granite forms more than 95 vol% of the known upper part of the Podlesí stock. It can be divided into two facies:

1. The "upper facies" occupies the uppermost 30–40 m of the cupola beneath the stockscheider (in borehole PTP-1). It is fine- to medium-grained (0.2–1.0 mm) and contains scarce Kfs phenocrysts. Albite (17–19 vol%) occurs as euhedral lamellar tablets. K-feldspar (35–41 vol%) forms mainly short prismatic subhedral non-perthitic grains, whereas long prisms are twinned, often perthitic and euhedral. Quartz grains (30–34 vol%) are equidi-

mensional and anhedral. Mica (6.5–8 vol%) is protolithionite (in the sense of Weiss et al. 1993) and contains small grains of radioactive accessory minerals (Fig. 8b). Topaz (3–4 vol%) occurs as euhedral (Fig. 8a) to subhedral grains with quartz inclusions. Early Mn-poor apatite prevails among the accessories (Fig. 8b). This facies probably represents a rapidly cooled and crystallised carapace of the granite body. This is in accordance with the relatively simple internal structure of all major minerals without significant zoning.

2. The "lower facies" is equigranular and medium-grained (1–2 mm) (Fig. 7a). The mineral composition is similar to that of the "upper facies", but all the major minerals show more complicated internal structure reflecting a longer period of crystallisation and interaction with fluids. Scarce late interstitial tourmaline aggregates were found in the deeper part of borehole PTP-1.

The stock granite near the layers of "dyke granite" is similar to the "lower facies", but reflects a more pronounced interaction with late-stage magmatic fluids. In one place in this area, the granite contained a layer with UST consisting of a finely-crystallised quartz layer about 1.5 cm thick accompanied by a 3 cm thick layer of oriented columns of orthoclase (Fig. 5d).

Dyke-like apophysis of the stock granite

A dyke of fine-grained albite-protolithionite granite outcrops near the SW contact of the granite stock. This 20 cm thick dyke crosses (dips 45° to the NE) the schistosity of folded phyllite. A layer of stockscheider up to 5 cm thick developed along the upper margin of this dyke.

Tab. 1. Whole-rock chemical analyses of outcropping granites (major elements in wt% by wet chemistry in laboratory of CGS Praha, trace elements in ppm by ICP-MS in laboratory ACME Vancouver).
Remarks:
3359 – aplite-like dyke of the stock granite intruding phyllite, near SW contact of the granite stock,
3361 – marginal pegmatite (stockscheider) at the SW contact of the granite stock,
3385 – stock granite, blocks near the S contact of the granite stock,
3365 – biotite-topaz-apatite greisen (greisenised stock granite), blocks near the S contact of the granite stock,
3389 – Li-mica greisen (greisenised dyke granite), block near the S contact of the granite stock,
3413 – fine-grained dyke granite, lower part of the major dyke in the quarry,
3416 – laminated dyke granite, upper part of the major dyke in the quarry.
3417 – Kfs-dominated UST-layer, upper part of the major dyke in the quarry.

	stock granite				dyke granite			
Rock type	aplite dyke	marginal pegmatite	stock granite	Bi-rich greisen	Li-mica greisen	lower part of the dyke	laminated dyke	UST layer
No.	3359	3361	3385	3365	3389	3413	3416	3417
SiO_2	71.76	74.78	73.8	70.56	83.52	72.52	70.1	66.54
TiO_2	0.04	0.05	0.06	0.04	0.05	0.01	0.02	0.02
Al_2O_3	15.28	13.8	14.58	14.71	11.63	15.98	15.77	17.79
Fe_2O_3	0.278	0.414	0.303	0.593	0.256	<0.01	0.111	0.15
FeO	0.632	0.464	0.879	4.6	0.256	0.55	0.674	0.945
MnO	0.034	0.026	0.015	0.088	0.022	0.041	0.036	0.046
MgO	0.02	0.05	0.04	0.02	0.01	0.04	0.02	0.02
CaO	0.56	0.43	0.39	0.6	0.28	0.17	0.43	0.39
Li_2O	0.163	0.033	0.125	0.445	0.071	0.29	0.332	0.442
Na_2O	4.13	3.6	3.19	0.08	0.03	4.89	4.1	2.9
K_2O	3.95	4.23	4.46	2.63	0.3	3.51	4.25	6.42
P_2O_5	0.705	0.397	0.375	0.479	0.326	0.524	1.03	0.8
CO_2	0.02	0.03	0.01	0.01	0.01	0.01	0.01	0.01
C	<0.005	0.007	<0.005	<0.005	<0.005	<0.005	0.011	0.007
F	1.34	0.505	1.28	4.34	3.46	1.33	1.31	1.72
S	<0.005	<0.005	0.008	0.014	0.005	<0.005	<0.005	<0.005
H_2O^+	0.887	0.884	0.96	2.35	1.11	0.901	1.34	1.55
H_2O^-	0.11	0.23	0.18	0.13	0.06	0.14	0.21	0.12
Total	99.36	99.72	100.13	99.87	99.96	100.36	99.22	99.16
Ba	36	23	15	29	73	9	13	12
Cs	68	56	149	253	30	159	143	198
Ga	46	31.4	33.4	59.5	5.8	51.9	59.9	56
Hf	2.6	2	2.2	2.2	2.4	1.8	4.6	2.2
Nb	60	57.6	28	37.7	18.5	54.4	93.1	79.4
Rb	1375	672	1229	1752	249	2010	2021	2754
Sn	23	20	16	65	19	35	23	31
Sr	120	12	38	155	168	53	167	87
Ta	36.8	18.7	8.3	14.1	10.5	19.6	68.3	53.9
Th	5.6	7.5	6.2	5.2	6.8	6.3	5.4	12.1
Tl	3.6	2.5	4.7	4.3	0.4	3.5	4.3	6.2
U	13	42.9	43.8	13.8	31.7	12.7	36.1	28.8
W	37	24	43	99	90	23	49	55
Zr	30.2	31	37.6	25.9	36.7	25.4	40	20.8
Y	3.5	8.5	11.1	6.7	11.2	2.3	2.2	2.8
Mo	1	<1	1	1	1	<1	<1	1
Cu	10	3	2	2	3	1	1	2
Pb	3	7	4	5	4	3	3	<3
Zn	41	20	48	181	22	49	56	65
As	25	11	13	7	3	5	9	11
Bi	42	2.8	4	82	717	8	8	49
La	1.2	2.4	2.9	1.4	2.7	0.7	< 0.5	0.7
Ce	2.7	5.6	7	3.6	7.3	1.7	1	1.7
Pr	0.3	0.71	0.87	0.47	0.84	0.2	0.17	0.25
Nd	1.1	2.5	3.4	1.8	3.1	0.8	1.1	1.1
Sm	0.3	1.1	1.2	0.8	1.1	0.2	0.3	0.5
Eu	<0.05	0.06	<0.05	<0.05	<0.05	<0.05	0.06	<0.05
Gd	0.41	1.1	1.32	0.83	1.51	0.26	0.41	0.48
Tb	0.1	0.31	0.32	0.23	0.4	0.04	0.05	0.08
Dy	0.61	1.73	2	1.24	2.29	0.29	0.33	0.4
Ho	0.08	0.22	0.27	0.15	0.31	<0.05	<0.05	0.05
Er	0.22	0.52	0.67	0.37	0.76	0.13	0.12	0.16
Tm	0.05	0.05	0.07	<0.05	0.09	<0.05	<0.05	<0.05
Yb	0.21	0.45	0.52	0.32	0.64	0.13	0.11	0.13
Lu	0.03	0.06	0.06	0.04	0.09	<0.01	0.01	0.01

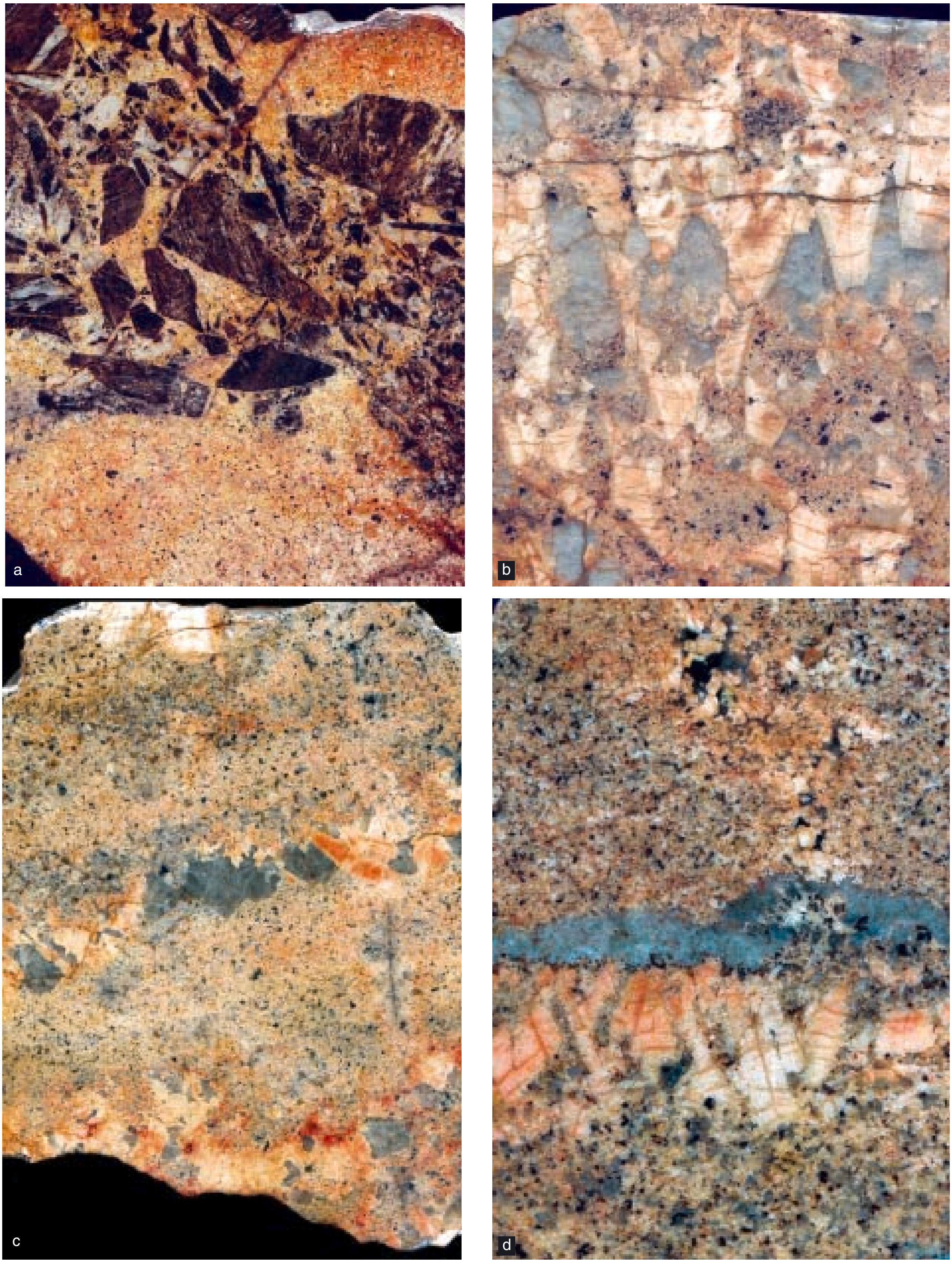

Fig. 5. Macrotextures of the stock granite (in cases b-d crystallisation from top to bottom): a – breccia, b – stockscheider, c – stockscheider-stock granite transitional zone, d – stock granite with UST layer. Scales 1 : 1.

→ Fig. 6. Macrotextures of the dyke granite (quarry, direction of crystallisation downwards): a – upper laminated layer with transition to the Kfs-dominated UST-layer; b – folded Q-Afs-Tp laminas (light) with zinnwaldite laminas (dark) and individual small comb quartz and large orthoclase crystals. In the lower right corner apatite aggregates (dark brown). Scales 1 : 1.

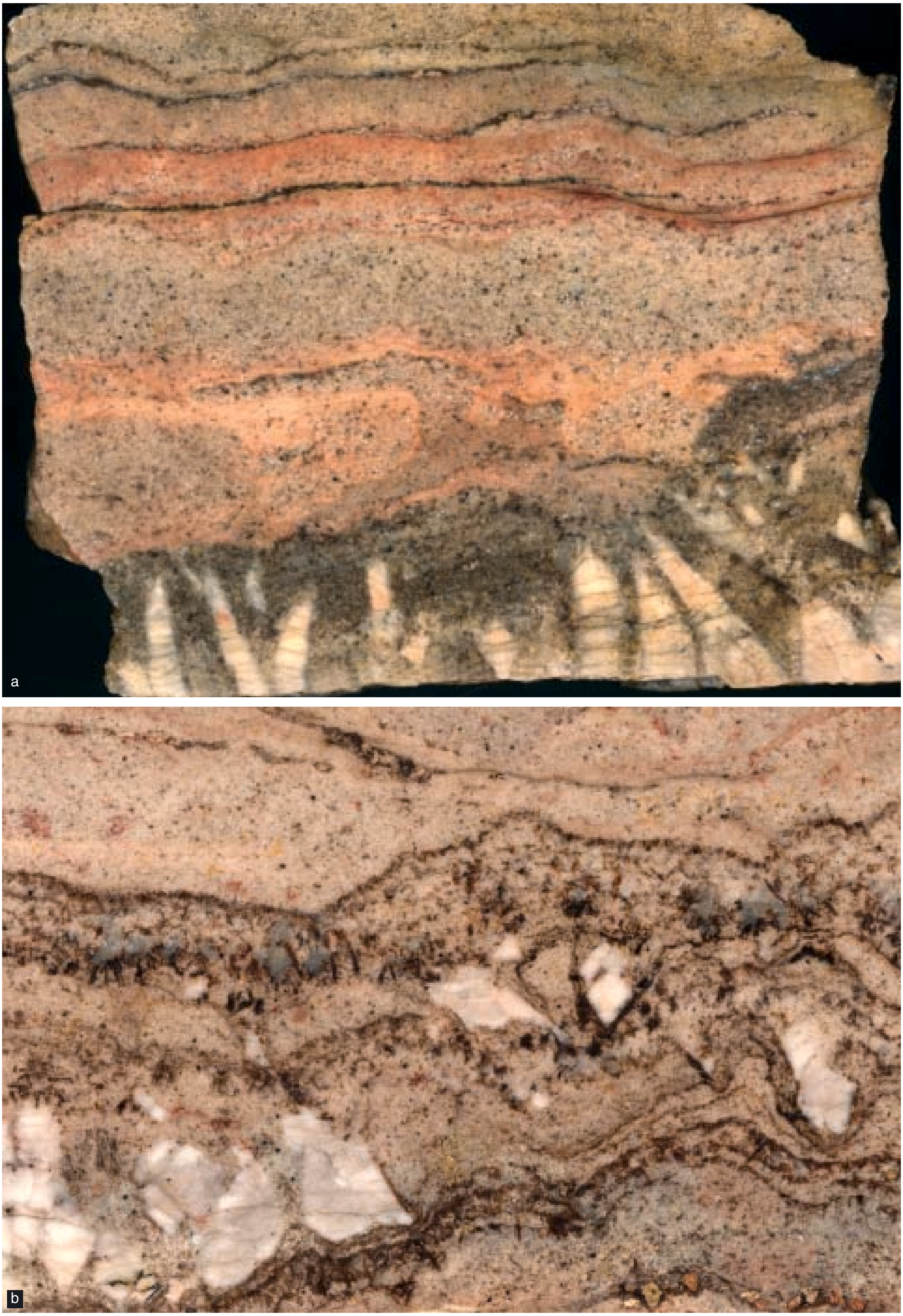
a
b

Tab. 2. Whole-rock chemical analyses of granites in deeper part of the borehole PTP-1 (major elements in wt% by wet chemistry in laboratory of CGS Praha, trace elements in ppm by ICP-MS in laboratories GFZ Postdam and ACME Vancouver).

Depth (m)	55.0	67.5	77.5	78.0	78.1	78.5	80.1	82.1	84.1	84.6	85.0	86.3	89.6	93.6	94.6	108.0	137.0	154.0	184.0	216.0	260.0	309.0
Rock type	stock granite	stock granite	stock granite	dyke granite	UST layer	dyke granite	dyke granite	dyke granite	dyke granite	dyke granite	stock granite	dyke granite	stock granite	dyke granite	stock granite	stock granite	dyke granite	stock granite	stock granite	stock granite	stock granite	stock granite
No.	2708	2704	2648	2649	2650	2651	2653	2655	2657	2658	2659	2662	2665	2669	2670	2677	3430	3432	3435	3438	3441	3445
SiO_2	74.05	73.8	73.27	71.73	67.31	72.55	72.58	71.70	70.98	68.8	73.53	72.10	73.81	71.86	72.81	72.97	72.52	72.9	73.10	73.94	73.08	74.10
TiO_2	0.07	0.06	0.05	0.02	0.02	0.03	0.05	0.02	0.03	0.02	0.05	0.02	0.06	0.03	0.03	0.03	0.04	0.06	0.04	0.06	0.03	0.05
Al_2O_3	14.08	13.98	14.19	15.46	17.5	14.74	14.75	15.05	15.39	15.94	14.59	15.31	13.97	15.19	15.08	14.66	14.10	13.92	14.26	13.79	14.7	14.28
Fe_2O_3	0.66	0.49	0.12	0.18	0.15	0.23	0.1	0.24	0.21	0.39	0.25	0.23	0.32	0.36	0.16	0.20	0.245	0.301	0.208	0.252	0.199	0.238
FeO	0.45	0.66	0.92	0.63	0.60	0.80	0.84	0.90	0.88	1.10	0.82	0.71	0.75	0.86	0.83	0.65	0.76	0.80	0.65	0.88	0.73	0.74
MnO	0.022	0.019	0.027	0.048	0.052	0.117	0.037	0.136	0.141	0.188	0.029	0.059	0.036	0.081	0.027	0.028	0.054	0.028	0.022	0.026	0.027	0.027
MgO	0.05	0.06	0.07	0.02	0.02	0.03	0.04	0.03	0.02	0.04	0.04	0.02	0.05	0.03	0.03	0.04	0.02	0.05	0.04	0.08	0.05	0.05
CaO	0.42	0.55	0.42	0.34	0.29	0.58	0.64	0.23	0.16	0.22	0.42	0.22	0.36	0.22	0.48	0.39	0.31	0.33	0.47	0.42	0.44	0.38
Li_2O	0.174	0.191	0.195	0.269	0.317	0.203	0.266	0.351	0.325	0.369	0.224	0.271	0.238	0.457	0.264	0.258	0.265	0.17	0.195	0.132	0.136	0.142
Na_2O	3.99	4.17	3.93	4.26	3.18	3.78	3.92	4.28	4.32	4.70	3.85	3.5	3.73	4.09	3.79	3.96	3.90	3.84	3.96	3.47	3.49	3.81
K_2O	4.31	4.11	4.30	3.90	7.57	3.96	4.25	3.95	4.13	4.64	4.2	5.47	4.37	3.71	4.43	4.35	3.97	4.45	4.29	4.35	4.39	4.36
P_2O_5	0.435	0.424	0.445	0.652	0.819	0.623	0.707	0.866	0.787	0.821	0.528	0.62	0.46	0.988	0.642	0.549	0.513	0.442	0.49	0.38	0.431	0.399
F	1.135	0.861	1.096	1.421	1.571	1.425	1.168	1.524	1.73	1.962	1.25	1.834	1.294	1.847	1.666	1.532	1.68	1.21	1.22	0.969	1.07	0.898
H_2O^+	0.76	0.90	0.84	0.87	0.92	0.97	1.04	0.96	0.96	1.09	0.84	0.99	0.79	1.13	0.99	0.97	0.889	0.881	0.964	0.94	0.973	0.784
H_2O^-	0.07	0.09	0.11	0.09	0.08	0.14	0.14	0.14	0.11	0.09	0.12	0.08	0.11	0.1	0.11	0.08	0.05	0.06	0.09	0.10	0.06	0.07
TOTAL	100.00	100.00	99.52	99.29	100.21	99.88	100.04	99.74	99.45	99.54	100.22	100.66	99.80	100.00	100.64	100.02	98.60	98.93	99.48	99.38	99.36	99.57
Ba	7.2	8.5	16.1	3.7	8.2	6.3	2.2	6.7	21.5	2.5	3.5	4.8	3.8	81.4	3.2	4.4	3	7	6	13	5	8
Cs	143	134	151	97.3	170	87.2	130	140	144	119	126	155	143	123	116	117	98.9	196.7	82.8	110.4	76.1	98.5
Ga	n.a.	n.a.	n.a.	n.a.	n.a.	n.a.	n.a.	n.a.	n.a.	n.a.	n.a.	n.a.	n.a.	n.a.	n.a.	n.a.	38	36.3	39.7	32.3	36.1	32.4
Hf	2.32	2.24	2.33	2.12	1.47	2.34	2.38	2.91	2.07	2.17	2.78	2.56	2.72	2.99	2.38	2.21	1.9	2.2	1.8	2.1	1.5	1.5
Nb	33	37	28	65	64	73	49	71	83	94	30	72	30	69	54	45	44.4	30.1	41.5	28.1	37	32
Rb	1203	1103	1226	1745	3000	1712	1671	1828	1962	1863	1496	1820	1546	1937	1750	1622	1646.7	1326.9	1519.2	1106.3	1188.2	1197.6
Sn	22	129	12	5	14	8	14	16	20	16	8	29	8	5	18	47	38	57	68	39	72	56
Sr	19	67	20	37	31	17	30	26	< 7	10	< 7	17	< 7	196	31	51	4.5	6.6	23.8	13.1	21.1	11.8
Ta	11	11	10	22	43	54	28	49	35	45	12	58	9	47	27	18	18.5	14	16.9	10.6	16.8	9.2
Th	5.89	6.64	6.01	5.47	10.3	6.11	5.33	5.13	5.08	5.73	6.99	3.96	7.94	6.15	6.38	6.01	4.6	7.7	5.8	7.7	4.7	6
Tl	n.a.	n.a.	n.a.	n.a.	n.a.	n.a.	n.a.	n.a.	n.a.	n.a.	n.a.	n.a.	n.a.	n.a.	n.a.	n.a.	3.1	2.9	3.3	2.5	2.4	3.8
U	33.9	36.6	35.7	21.6	17	21.7	29.1	24	21.2	31.5	37.8	20.1	42.7	26.5	28.9	32	32.9	44.4	44.7	47	27.7	36.9
W	44	61	48	48	50	57	47	41	41	59	30	53	42	40	26	31	64	45	48	25	22	57
Zr	30	27	33	20	< 7	13	23	24	14	24	35	20	36	20	20	23	29.9	41.1	30.9	41.4	27.3	30.9
Y	9.18	9.43	9.97	2.22	0.565	1.65	6.27	2.19	1.31	1.41	10.3	1.11	10.7	1.34	5	5.97	7.2	11.2	7.8	11.3	6.6	8.5
Mo	< 7	< 7	< 7	< 7	< 7	< 7	< 7	< 7	< 7	< 7	< 7	< 7	< 7	< 7	< 7	< 7	1	< 1	< 1	< 1	1	1
Cu	< 7	< 7	< 7	< 7	< 7	< 7	< 7	< 7	< 7	< 7	< 7	< 7	< 7	< 7	< 7	< 7	1	< 1	1	1	2	2
Pb	5.24	5.08	5.17	3.18	3.53	2.74	3.94	2.29	-2	2.95	5.07	3.16	5.41	2.74	3.88	5.32	< 3	3	3	5	4	5
Zn	37	45	38	62	68	43	75	69	73	96	55	98	41	109	80	62	28	34	30	28	28	47
As	< 7	< 7	< 7	63	11	< 7	< 7	14	13	9	< 7	19	< 7	8	20	< 7	3	20	2	4	< 2	44
Bi	n.a.	n.a.	n.a.	n.a.	n.a.	n.a.	n.a.	n.a.	n.a.	n.a.	n.a.	n.a.	n.a.	n.a.	n.a.	n.a.	63.5	1.9	3.4	0.6	9.1	0.6
La	2.80	2.42	2.26	0.453	0.123	0.35	1.41	0.45	0.29	0.284	2.47	0.327	2.84	0.369	1.18	1.37	1.4	3.8	1.9	3.9	1.7	3.1
Ce	5.42	6.22	5.76	1.20	0.26	0.872	3.69	1.15	0.64	0.705	6.44	0.752	7.42	0.863	3.07	3.74	4	10	5.1	10.1	4.5	7.9
Pr	0.71	0.814	0.756	0.149	0.024	0.111	0.49	0.151	0.076	0.082	0.848	0.093	0.966	0.106	0.408	0.474	0.51	1.16	0.63	1.2	0.52	0.95
Nd	2.36	2.74	2.52	0.481	0.08	0.349	1.58	0.484	0.234	0.242	2.77	0.317	3.18	0.342	1.35	1.6	1.7	4.3	2.2	4	1.8	3.3
Sm	0.961	1.03	0.974	0.232	0.039	0.156	0.687	0.249	0.108	0.113	1.1	0.108	1.26	0.147	0.578	0.657	0.7	1.4	0.9	1.3	0.7	1.2
Eu	0.014	0.012	<0.01	<0.01	<0.01	<0.01	<0.005	<0.005	<0.005	<0.01	<0.01	<0.01	<0.03	<0.03	<0.03	<0.01	< 0.05	< 0.05	< 0.05	< 0.05	< 0.05	< 0.05
Gd	1.15	1.3	1.28	0.263	0.055	0.186	0.786	0.249	0.116	0.137	1.34	0.137	1.46	0.16	0.622	0.785	0.71	1.44	0.95	1.37	0.71	1.16
Tb	0.302	0.315	0.341	0.072	0.012	0.044	0.204	0.067	0.034	0.035	0.343	0.032	0.361	0.034	0.16	0.197	0.21	0.32	0.25	0.36	0.2	0.3
Dy	1.78	1.91	1.97	0.436	0.07	0.284	1.19	0.384	0.208	0.236	2.03	0.199	2.2	0.242	0.984	1.192	1.17	1.89	1.29	1.95	1.07	1.58
Ho	0.273	0.278	0.291	0.056	0.012	0.042	0.175	0.058	0.031	0.034	0.297	0.03	0.325	0.037	0.151	0.165	0.2	0.32	0.2	0.31	0.18	0.23
Er	0.621	0.62	0.69	0.149	0.035	0.106	0.393	0.138	0.085	0.085	0.695	0.076	0.743	0.088	0.345	0.424	0.51	0.91	0.54	0.84	0.49	0.65
Tm	0.082	0.084	0.098	0.023	0.008	0.019	0.065	0.024	0.014	0.013	0.097	0.012	0.108	0.015	0.055	0.062	0.07	0.13	0.08	0.11	0.06	0.08
Yb	0.519	0.516	0.588	0.171	0.055	0.145	0.41	0.174	0.114	0.124	0.6	0.101	0.641	0.116	0.336	0.419	0.46	0.69	0.53	0.68	0.44	0.54
Lu	0.069	0.063	0.079	0.021	0.008	0.017	0.048	0.019	0.015	0.016	0.077	0.013	0.082	0.014	0.037	0.05	0.06	0.08	0.06	0.08	0.06	0.06

Dyke granite

The following description of dyke granite is based on an excellent outcrop in the old quarry. A magmatically layered dyke with both contacts is exposed over a length of 25 m and a thickness of up to 7 m (Figs 4, 6). The dyke is comprised of the following layers (from top to bottom):

1. a fine-grained uppermost layer 1cm thick in sharp contact with the hangingwall stock granite.
2. a Kfs-rich layer 2–3 cm thick consisting of columnar crystals of Kfs oriented perpendicular to the contact and infilled with fine-grained albite-zinnwaldite-topaz matrix.
3. a fine-grained laminated layer about 30 cm thick: thin laminae consist of quartz, albite and P-rich Kfs in variable proportions; individual laminae have sharp contacts (Fig. 8f). Zinnwaldite is partly disseminated, partly concentrated in nearly monominerallic laminae composed of fan-like aggregates (Fig. 8d). Contacts of these laminae are generally irregular and/or folded (Fig. 7c). Small-scale protrusions of some laminae into their hanging wall appear to have formed before the laminae were fully crystallised.
4. a pegmatite-like layer about 10 cm thick consists of large (up to 7 × 1 cm) oriented subhedral columns of twinned orthoclase (Fig. 7d) rimmed by fan-like aggregates of zinnwaldite. The fine-grained granitic matrix is composed of rounded phenocrysts of snow-ball quartz (Fig. 8e), anhedral quartz, K-feldspar, albite and zinnwaldite. Topaz is common.
5. a laminated fine-grained layer, 15 cm thick, with scarce comb quartz. This layer is enriched in strontium and contains late-stage phosphate minerals. Intergrowths of zinnwaldite with apatite and small nests of pegmatite with tourmaline (1–2 cm in diameter) are typical.
6. the rest of the dyke (ca. 90 vol% of the whole dyke) is homogeneous, fine-grained (0.1–0.5 mm) with scarce Kfs phenocrysts (Fig. 7b). Quartz (22–34.5 vol%), K-feldspar (33.5–39.5 vol%) and albite (18–26 vol%) grains are generally anhedral; both types of feldspar also occur as short subhedral prisms. Some quartz grains have prominent snow-ball texture. Rims of many larger feldspar grains are leached and replaced by late quartz, albite and topaz. Grains of quartz, K-feldspar, mica and topaz are markedly zoned. The mica, zinnwaldite (6.5–8 vol%), forms subhedral flakes. Topaz (3.5–6 vol%, 0.3–0.5 mm across) occurs as large subhedral to euhedral crystals and as small interstitial grains. Phosphate minerals, apatite, amblygonite and childrenite (up to 1 vol%), are the most common accessory minerals.

The thin dykes (20–100 cm thick) are homogeneous, fine-grained, with mineral composition similar to that of the lower part of the major dyke.

Greisens

Evidence of hydrothermal alteration is scarce. The dyke granite exposed in the quarry has been altered to quartz-rich greisen with traces of Li-mica, topaz and wolframite in some places.

Thin, steep stringers of dark greisen are present within the stock granite in the outcrop and in boreholes down to the depth of more than 300 m. The dark greisen consists of quartz (old granitic, and young formed during greisenisation), Fe- and F-rich and Li-poor mica, and relicts of feldspars, topaz and apatite. Scarce stringers of biotite-rich greisen were found also in the older biotite granite in boreholes PTP-3 and PTP-4a.

Whole-rock chemistry

Representative whole-rock chemical analyses are presented in tables 1–3; relationships between chemical elements are shown on figure 9.

The stock granite is strongly peraluminous (A/CNK 1.15–1.25). Compared to common Ca-poor granites, it is strongly enriched in incompatible elements such as Li, Rb, Cs, Sn, Nb, W, and poor in Mg, Ca, Sr, Ba, Fe, Sc, Zr, Pb, and V. It is also relatively rich in phosphorus (0.4–0.8 wt% P_2O_5) and fluorine (0.6–1.8 wt% F). A high degree of magmatic fractionation is reflected by low K/Rb and Zr/Hf ratios (22–35 and 12–20, respectively) and high U/Th ratio (4–7).

The more evolved dyke granite is even more enriched in Al (A/CNK 1.2–1.4), P (0.6–1.5 wt% P_2O_5), F (1.4–2.4 wt%), Na, Rb, Li, Nb, Ta, and depleted in Si, Zr, Sn, W and REE. The K/Rb (14–20) and Zr/Hf (9–13) ratios are lower than those in the stock granite.

The layered upper part of the major dyke is chemically inhomogeneous and reflects rapid changes in composition of crystallised melt in an open system (Table 4).

The stock granite within the dyke-rich zone (depth 78–120 m in borehole PTP-1) is also enriched in Al, P, F, Mn, Li, Rb, Cs, Nb, Ta, and depleted in Si, Zr and REE relative to its roof and bottom zones. This can be explained by the influence of fluids that migrated from the dykes into the neighbouring stock granite. Nevertheless, the differences between the stock granite and the dyke granite are distinct.

All phases of the granite are rich in phosphorus, which shows a positive correlation with F, Al, Li, Rb, Nb, Ta and peraluminosity, and negative correlation with Si, Zr and Sn. There is no correlation between P on one side, and Na, K, and Sr on the other (Breiter et al. 1997a, Breiter 2001b).

Few data exist about the content of boron, which ranges between 20 and 60 ppm. The primary B content in the melt must have been much higher, as suggested by intensive tourmalinisation (B contents of up to 5 000 ppm) evolved in broader exocontact in phyllite (unpublished data of CGS).

A high degree of fractionation is documented also by unusually high concentrations of rare metals. Nb and Ta are preferentially concentrated in the more peraluminous dyke granite (50–95 ppm Nb and 30–55 ppm Ta) com-

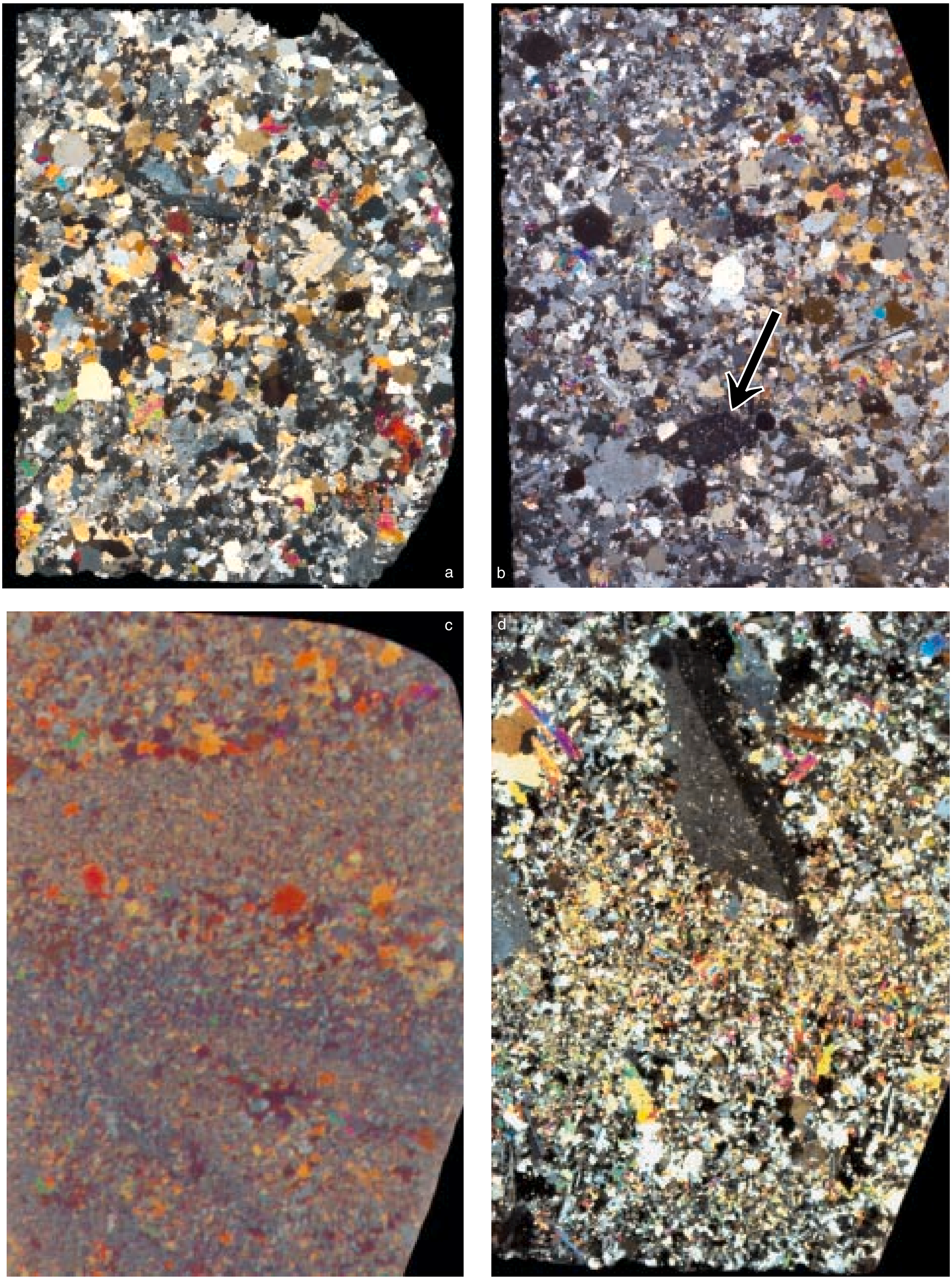

Fig. 7. Microtextures (area of all images is 30 × 20 mm, crossed polars): a – stock granite, borehole PTP-1, depth 300 m (No.2687), b – dyke granite, borehole PTP-1, depth 82.3 m (remember zoned Kfs phenocryst), c – laminated dyke granite, quarry, d – Kfs-dominated UST with Kfs phenocryst with zonally arranged Ab-inclusions (direction of the crystallisation downwards), dyke granite, quarry.

Tab. 3. Whole-rock chemical analyses of granites from the borehole PTP-3 (major elements in wt% by wet chemistry in laboratory of CGS Praha, trace elements in ppm by ICP-MS in laboratory ACME Vancouver).

Depth (m)	13.7	26.0	31.4	48.8	65.7	82.4	92.4	105.9	160.5	198.7	226.1	231.5	245.5	259.8	264.8	299.7	318.0	338.5	347.8
Rock type	dyke granite	stock granite	dyke granite	stock granite	stock granite	stock granite	biotite granite	biotite granite	biotite granite	biotite granite	biotite granite	stock granite	stock granite	stock granite	stock granite	stock granite	stock granite	stock granite	stock granite
No.	3399	3447	3449	3452	3455	3458	3461	3464	3471	3475	3478	3490	3492	3495	3496	3501	3504	3508	3511
SiO_2	72.10	72.32	72.28	71.52	73.51	73.22	73.64	73.72	74.02	73.56	73.62	73.78	72.55	71.60	72.56	74.04	72.62	72.4	72.58
TiO_2	0.04	0.05	0.05	0.03	0.04	0.05	0.04	0.06	0.07	0.05	0.07	0.04	0.04	0.03	0.04	0.04	0.04	0.04	0.06
Al_2O_3	15.46	14.93	14.88	15.48	14.21	14.78	14.22	14.41	13.92	14.34	14.23	14.57	14.71	15.57	14.54	14.57	14.9	15.01	14.82
Fe_2O_3	0.214	0.404	0.313	0.273	0.217	0.186	0.269	0.395	0.28	0.222	0.313	0.221	0.17	0.179	0.202	0.155	0.198	0.228	0.266
FeO	0.644	0.816	0.69	0.889	0.651	0.66	0.802	0.661	0.71	0.781	0.78	0.692	0.783	0.541	0.673	0.661	0.641	0.622	0.751
MnO	0.025	0.043	0.028	0.044	0.04	0.021	0.026	0.026	0.022	0.023	0.031	0.028	0.028	0.039	0.039	0.025	0.041	0.032	0.033
MgO	0.02	0.14	0.05	0.05	0.03	0.03	0.07	0.05	0.06	0.05	0.05	0.05	0.04	0.05	0.07	0.04	0.03	0.05	0.04
CaO	0.38	0.76	0.49	0.82	0.47	0.49	0.43	0.5	0.45	0.35	0.33	0.52	0.36	0.63	0.48	0.32	0.4	0.48	0.35
Li_2O	0.24	0.164	0.241	0.209	0.201	0.179	0.183	0.147	0.114	0.125	0.114	0.212	0.156	0.182	0.193	0.195	0.173	0.19	0.147
Na_2O	3.73	3.28	4.1	3.38	4	4.05	3.85	3.72	3.75	3.83	3.81	3.54	3.84	3.19	3.56	3.93	3.98	3.94	3.90
K_2O	3.94	4.31	4.28	4.2	4.22	4.07	4.23	4.28	4.36	4.5	4.55	4.21	4.32	4.46	4.36	3.88	3.92	4.15	4.15
P_2O_5	0.595	0.664	0.579	0.668	0.522	0.499	0.417	0.456	0.412	0.391	0.345	0.532	0.451	0.62	0.533	0.421	0.518	0.517	0.445
CO_2	0.01	0.014	< 0.01	0.016	0.014	< 0.01	< 0.01	< 0.01	0.013	< 0.01	< 0.01	< 0.01	< 0.01	< 0.01	< 0.01	< 0.01	< 0.01	< 0.01	< 0.01
F	1.69	1.1	1.31	1.77	1.06	1.23	1.09	1.11	1.04	0.772	0.65	1.63	1.45	1.65	1.28	1.5	1.32	1.23	1.33
H_2O^+	1.2	1.33	0.986	1.33	0.831	0.873	0.84	0.95	0.967	0.747	0.655	1.11	0.784	1.11	1.10	0.973	0.821	0.99	0.794
H_2O^-	0.19	0.23	0.05	0.11	0.11	0.1	0.13	0.12	0.09	0.1	0.06	0.04	0.05	0.08	0.10	0.07	0.07	0.14	0.08
Total	**99.77**	**99.63**	**99.2**	**99.23**	**99.23**	**99.38**	**99.31**	**99.67**	**99.4**	**99.23**	**99.12**	**100.49**	**99.13**	**99.24**	**99.2**	**100.19**	**99.13**	**99.52**	**99.19**
Ba	6	12	5	15	5	5	10	6	10	5	9	6	10	5	5	3	4	3	12
Cs	136	74	141	132	112	101	165	111	145	126	121	136	156	79	78	113	124	134	114
Ga	39.6	44	45.9	45	40.8	37	39.2	36.8	38.5	37.6	32	40.1	38.2	42.3	41	37.1	41.1	43.5	39.2
Hf	2.1	2.3	1.9	2.2	1.9	1.5	2.1	1.9	2.1	1.7	2.1	2.3	1.7	1.7	1.8	1.4	2.4	1.6	1.9
Nb	49	43	54	44	43	37	37	34	32	29	28	36	34	52	38	32	36	39	31
Rb	1561	1503	1766	1514	1574	1316	1520	1186	1175	1212	1066	1502	1326	1608	1456	1327	1255	1216	1270
Sn	16	44	22	37	51	63	48	47	58	39	51	73	54	202	52	70	81	95	57
Sr	7	231	58	170	35	29	29	24	22	10	4.9	26	11	21	15	19	24	28	11
Ta	22.8	22.9	23.4	19.2	17.3	16.6	14.1	12.3	14.6	16.4	8.2	19.3	18.1	27.4	17.2	12.8	14.1	18.3	11.8
Th	4.9	6.1	5.2	6.1	5.8	5.2	8.8	6.3	6.9	6.3	6.9	5.5	5.3	5.2	3.8	3.4	4.2	4.6	4.5
Tl	3.1	3.8	4.2	3.7	3.8	4.9	5.1	3.6	4	3	3.1	2.3	1.4	2.6	2.2	1.8	2.6	2.6	1.3
U	36	16.7	33	39	39	40	43	42	51	31	15.3	41	32	32	37	32	33	21	14.8
W	78	30	68	102	36	38	39	17	26	20	18	30	31	58	28	56	43	37	28
Zr	25	30	26	32	31	26	42	33	40	35	37	36	27	22	24	17	30	16	29
Y	6.5	7.2	5.5	8.2	6.9	6.7	10.7	8.7	10.4	9.6	9.7	6.8	7.6	7.9	5	4	8.5	7	7.4
Mo	< 1	< 1	1	14	1	< 1	< 1	< 1	1	< 1	1	1	< 1	< 1	< 1	< 1	< 1	< 1	1
Cu	< 1	4	1	3	< 1	< 1	< 1	< 1	1	1	1	3	2	2	2	2	1	1	1
Pb	< 3	4	< 3	3	3	3	3	3	5	3	3	3	< 3	< 3	< 3	< 3	< 3	< 3	< 3
Zn	46	35	42	53	38	32	32	27	25	23	23	32	27	28	40	37	29	45	36
As	9	4	11	44	23	7	15	4	9	11	9	12	20	7	6	19	11	11	9
Bi	31	4.6	16.8	218	12	8.4	8.3	1.1	3.3	0.5	2.5	5.7	2.6	12.1	3.6	4.6	2.9	6.4	4.3
La	1.0	1.8	1.3	1.9	1.7	1.7	3.8	2.2	2.7	2.7	3.3	1.4	1.9	1.3	1.1	0.9	1.4	1.7	2.1
Ce	3.1	4.8	3.3	4.9	4.5	4.3	9.8	5.8	7.0	6.4	8.4	4.5	5.3	4.3	2.9	2.4	4.3	4.4	5.4
Pr	0.38	0.58	0.43	0.65	0.56	0.55	1.25	0.71	0.85	0.76	0.96	0.57	0.64	0.59	0.39	0.3	0.59	0.56	0.7
Nd	1.4	2.2	1.3	2.3	1.9	2.1	4.6	2.8	3.1	2.7	3.6	2.1	2.5	2.1	1.2	1.0	2.3	2.0	2.5
Sm	0.7	0.9	0.6	0.8	0.7	0.7	1.3	1.1	1.0	0.9	1.1	0.7	1.0	1.1	0.6	0.5	1.2	0.8	1.0
Eu	<0.05	< 0.05	< 0.05	< 0.05	< 0.05	< 0.05	< 0.05	< 0.05	< 0.05	< 0.05	< 0.05	< 0.05	< 0.05	< 0.05	< 0.05	< 0.05	< 0.05	< 0.05	<0.05
Gd	0.76	0.94	0.64	0.98	0.92	0.89	1.41	1.11	1.23	1.2	1.33	0.91	0.91	1.15	0.68	0.52	1.13	0.85	0.93
Tb	0.2	0.22	0.17	0.26	0.26	0.20	0.34	0.26	0.29	0.27	0.28	0.21	0.25	0.29	0.15	0.14	0.27	0.22	0.24
Dy	1.07	1.28	0.92	1.56	1.32	1.33	2.18	1.52	1.91	1.59	1.69	1.29	1.42	1.51	0.99	0.8	1.79	1.37	1.58
Ho	0.14	0.19	0.16	0.21	0.19	0.20	0.35	0.24	0.32	0.26	0.27	0.18	0.22	0.2	0.14	0.1	0.23	0.16	0.19
Er	0.38	0.53	0.38	0.59	0.50	0.51	0.80	0.56	0.74	0.66	0.77	0.43	0.52	0.46	0.31	0.27	0.58	0.46	0.54
Tm	< 0.05	0.06	0.05	0.07	0.06	0.06	0.10	0.08	0.10	0.09	0.09	0.06	0.06	0.06	0.05	< 0.05	0.09	0.07	0.07
Yb	0.42	0.45	0.37	0.49	0.44	0.41	0.58	0.45	0.66	0.6	0.61	0.46	0.51	0.48	0.36	0.29	0.59	0.49	0.51
Lu	0.05	0.05	0.04	0.05	0.05	0.05	0.07	0.05	0.08	0.07	0.07	0.05	0.05	0.05	0.04	0.03	0.07	0.06	0.07

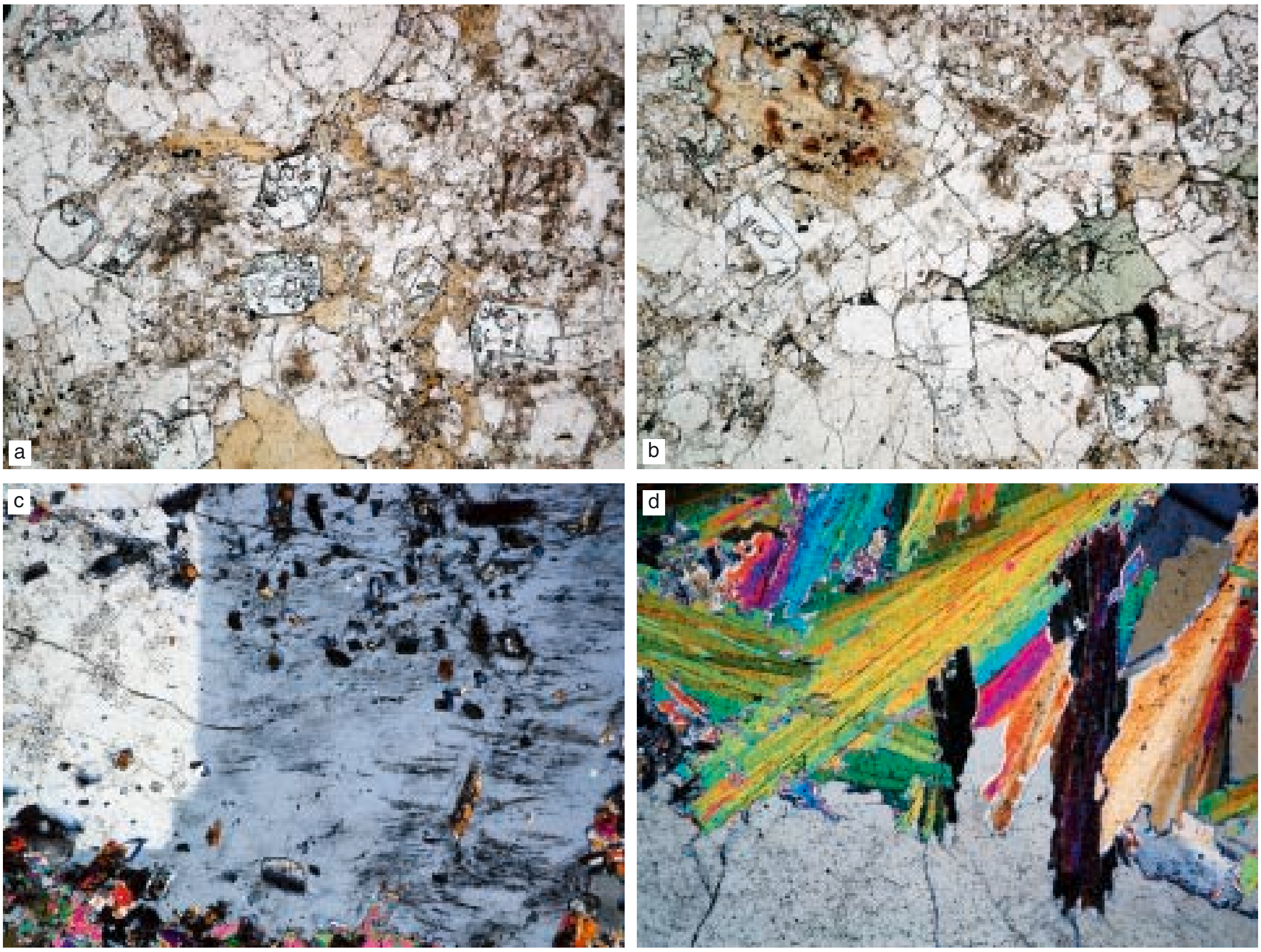

Fig. 8. Microphotos: a – stock granite, upper outcrop (No. 2754), topaz crystals with quartz inclusions, inclusions-free protolithionite, b – stock granite, upper outcrop (No. 2754), large green apatite with protolithionite rich in radioactive inclusions, c – dyke granite, quarry (No. 3647), Kfs phenocryst in the UST: the inner part is rich in albite inclusions, the rim is inclusion-free, d – laminated dyke granite, block E of the quarry (No. 3357), fan-like aggregates of zinnwaldite, direction of crystallisation downwards, e – laminated dyke granite, quarry (No. 3402b), snow-ball quartz phenocryst,

pared to the stock granite (25–50 and 10–25 ppm, respectively). On the other hand, contents of Sn and W are distinctly higher in the stock granite (10–50 ppm Sn, 20–80 ppm W) than in the dyke granite (5–20 ppm Sn and 35–60 ppm W).

Unusually high contents of Sr (and also Ba) in some samples from the layered part of the dyke granite in the quarry are probably a product of late re-equilibration with aqueous fluids.

The REE content of the stock granite is low. Chondrite-normalised patterns are relatively flat (Ce/Yb_{CN} = 4–5) with distinct negative Eu anomalies (Fig. 10). The dyke granite is even more depleted in REE and shows lanthanide tetrad effect (Breiter et al. 1997a).

Vertical distribution of P, F and Li is demonstrated on logs of boreholes PTP-1 (Fig. 11a) and PTP-3 (Fig. 11b). Inside the stock granite, P, F and all the volatile elements are enriched in its upper part (with exception of the first 20–30 m under the contact with phyllite). The dyke granite is even more P, F and volatile-rich, although within the dyke system, the deeper dykes are relatively less enriched. Enrichment of P, F and volatile elements in upper part of the stock granite intrusion in comparison with its lower part, and even stronger enrichment of these elements in the dykes of the dyke granite, is clearly evident.

Mineralogical remarks

Alkali feldspars

Alkali feldspars from the Podlesí system are described in detail elsewhere (Breiter et al. 2002); only a brief recapitulation is presented here. Alkali feldspars are represented by nearly pure end members in the whole system – albite (<3% An) and Kfs (<5% Ab). The Kfs are more interesting from genetic point of view. The following types of Kfs can be distinguished:

1. Kfs1: this type is represented by phenocrysts with perthitic cores and homogeneous rims. Kfs1 is com-

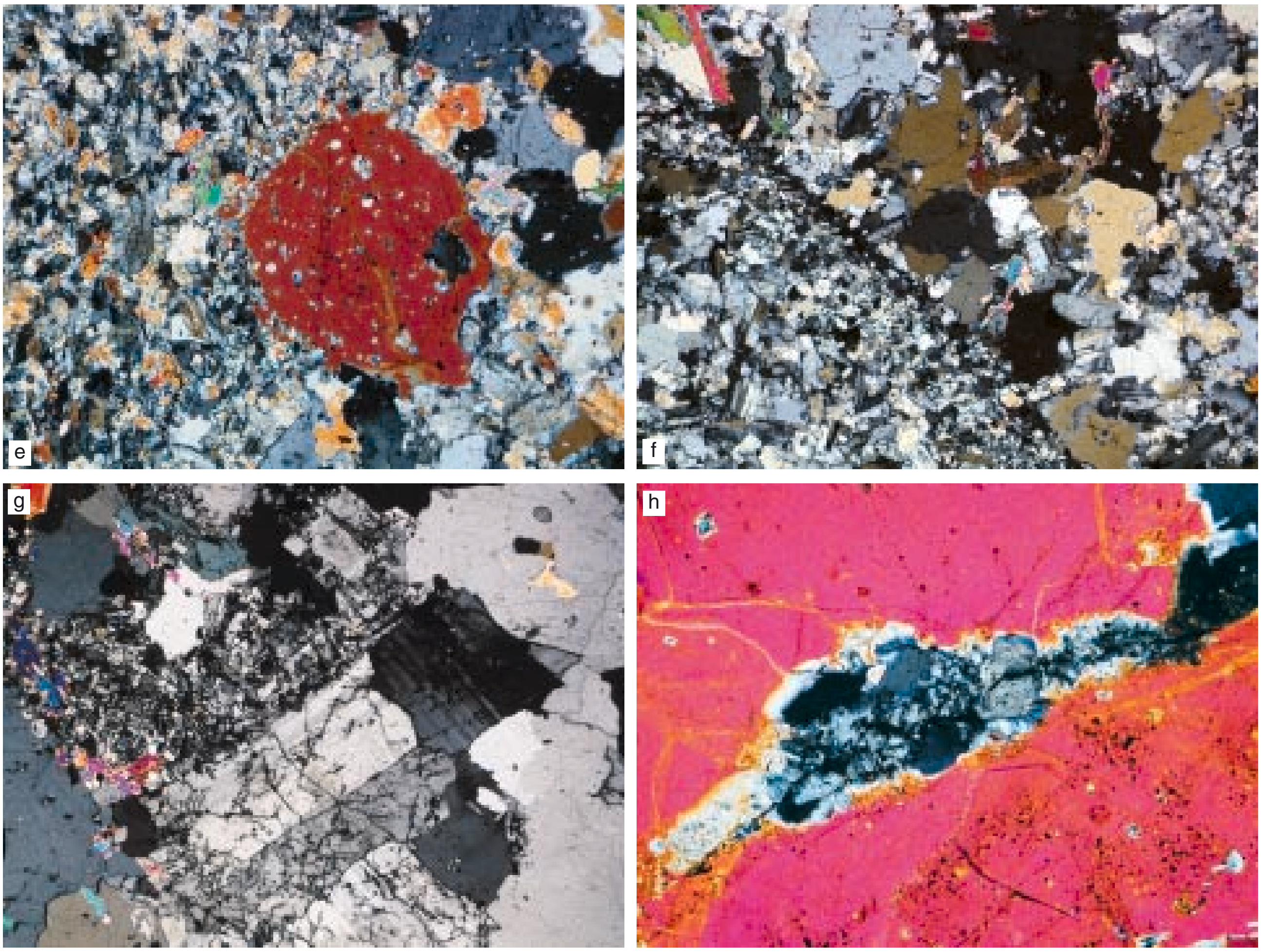

f – laminated dyke granite, quarry (No. 3480H), sharp limit of individual laminas, direction of crystallisation right upwards, g – upper contact of the major dyke with the stock granite in the quarry (No. 3536), small invasion of residual dyke granite melt into stock granite, h – dyke granite near the upper contact of the major dyke in the quarry (No. 3537), residual melt crystallised within brittle join in quartz phenocryst.
Area of image 8h is 1.4 × 1.0 mm, area of all other images is 3.5 × 2.5 mm. Images 8c-8h are in crossed polars.

mon in the stock granite, but scarce in the dyke granite. It contains 0.15–0.20% Rb and about 0.4% P_2O_5.

2. Kfs2: non-perthitic Kfs is the most abundant type. It is homogeneous in the stock granite, and zoned with P-enriched rims in the dyke granite (0.8–1.5% P_2O_5, 0.3% Rb in the stock granite, 0.5% Rb in the dyke granite, up to 0.7% Rb in the laminated part of the major dyke).
3. Kfs3: this type forms large crystals in the stockscheider. The inner parts of the crystals are moderately enriched in phosphorus (0.6–0.8% P_2O_5); the outer zones have been partially leached and depleted in phosphorus (0.1–0.3% P_2O_5) and contain many small admixtures of apatite vissible in the cathodoluminiscent (CL) images. Among all Kfs types, only Kfs3 is triclinic.
4. Kfs4: this type is represented by large crystals from the UST layer of the dyke granite. These crystals typically have macroscopically visible zones with dominant pale cores upon which thin (2 mm) colourless rims have developed. Microscopically, the core zone is homogeneous; the transitional zone contains numerous inclusions of small albite crystals oriented parallel to the growth zones of Kfs, whereas the rim is again homogeneous (Fig. 8c). No apatite occurs within the Kfs crystals. This type of Kfs contains 0.3–0.4% Rb and 0.6–0.8% P_2O_5.

Quartz

Quartz was studied in detail by Müller et al. (2001, 2002). The following types of quartz were distinguished according to the inner structure and contents of trace elements:

1. Q1: phenocrysts in the stock granite; this type is rich in Ti, similar to phenocrysts in rhyolites, and probably formed at great depth,
2. Q2: groundmass quartz in all granite types, likely formed *in situ*,
3. Q3: snowball quartz and comb quartz; this type, common in the dyke granite, is rich in Al and formed *in situ* (Fig. 8e).

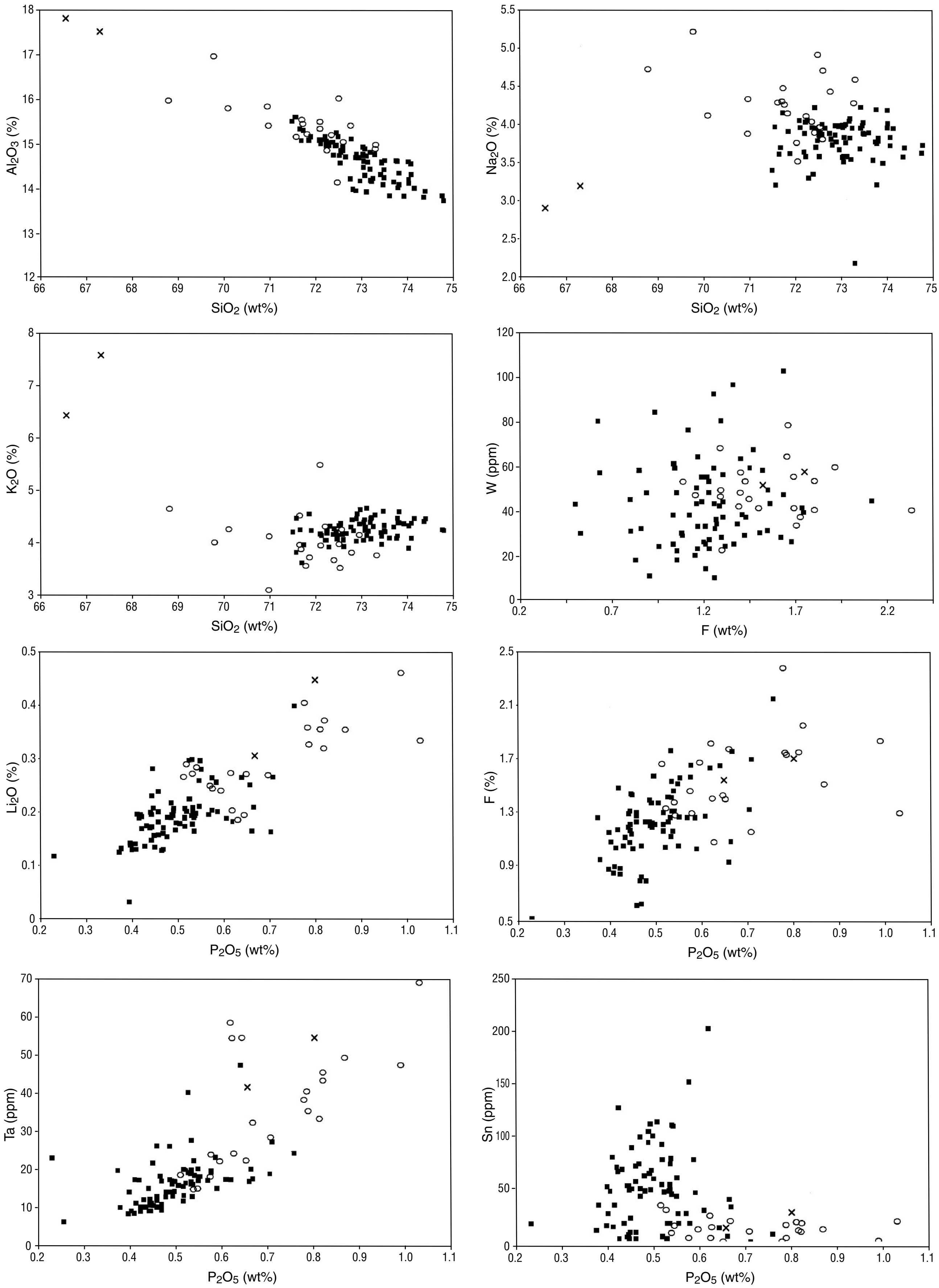

Fig. 9. Variation of selected major and trace element concentrations for Podlesí granite system. Remember positive correlation among P_2O_5, F, Li_2O and Ta. Explanatory notes: full squares – stock granite, open circles – dyke granite, crosses – UST domains.

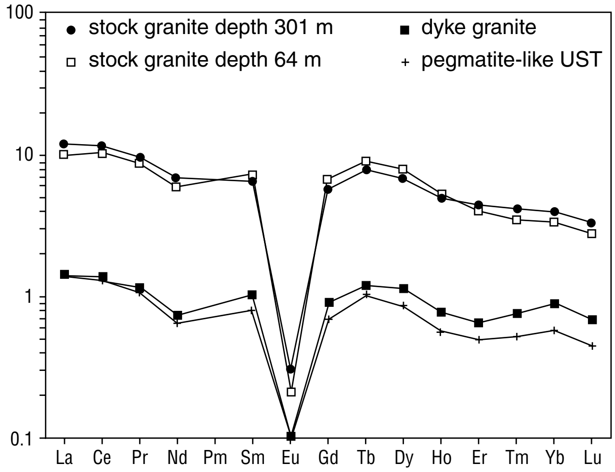

Fig. 10. Chondrite-normalised distribution patterns of REEs in typical samples from borehole PTP-1.

Li-rich micas

Mica is the only mafic mineral in all granite types. In all samples, micas are represented by F-rich Li-Fe trioctahedral micas, whose chemical composition differs depending on the host granite type (Skála et al. 1998) (Table 5).

Mica in the stock granite is generally protolithionite (in the sense of Weiss et al. 1993). Crystals of protolithionite are homogeneous, with no internal zoning. In many places, they contain small grains of radioactive minerals with pleochroic haloes (Fig. 8b). Fluorine contents reach 5–7 wt%.

The dyke granite and the adjacent stock granite contain zinnwaldite. Zinnwaldite flakes are distinctly zoned, with cores enriched in Fe, Mg and Ti, and rims higher in Si and Li (Li contents were calculated using the method of Tindle and Webb (1990), and are in overall agreement with analyses of mica separates by AAS). In contrast, there is no zoning in F, Rb and Cs (Breiter et al. 1997a and new data). Spectacular fan-like aggregates of zinnwaldite occur within the layered and UST-rich parts of the dykes (Fig. 8d).

Fluorine contents in profiles across zinnwaldite crystals are not less than 8 wt%, indicating that fluorine atoms almost completely occupy the OH-F sites. Zinnwaldite crystals with fluorine oversaturation were found in the dyke granite. This phenomenon has been reported from laboratory experiments, but not yet from natural micas (M. Rieder, personal communication).

Zinnwaldite and protolithionite grains analysed by EMPA can be effectively distinguished by means of the Si-Fe plot (Fig. 12). Li-rich zinnwaldite is relatively enriched in Al and depleted in Fe, which corresponds well with the whole-rock chemistry of parental rocks (Breiter et al. 1997a, Skála et al. 1998).

About 40 samples of mica concentrates (purity (99%) were analysed by wet methods for the contents of Li, F and trace elements Rb, Cs, Be, Sr, Ba, and Zn (Tab. 5).

Tab. 4. Partial chemical composition (in wt%) of individual laminas in sample 3402b (WR-analyse No.*3416*) from the upper part of the major dyke in the quarry. Location of analysed domains see on Fig. 15b. (EMPA, defocused EDS-analyses in laboratory CGU Praha).

Domain	V	W	X	Y	Z
SiO_2	77.9	70.9	71.3	68.9	69.4
Al_2O_3	13.0	17.8	17.4	16.6	18.4
FeO	0.4	0.1	0.6	0.2	0.2
CaO	0.0	0.1	0.0	0.0	0.0
Na_2O	5.1	8.4	6.9	1.7	7.7
K_2O	3.0	1.8	3.1	11.4	3.1
P_2O_5	0.4	0.7	0.6	1.2	1.0
Na_2O/K_2O	1.7	4.7	2.2	0.1	2.5

Variations in the chemistry of Li-Fe micas is a good indicator of vertical zoning in the granite body in borehole PTP-1 and of the contacts between individual intrusions within the core of borehole PTP-3 (Fig. 13). The F- and Li-contents of trioctahedral micas correspond well with those of whole rocks (Figs 13 and 11b).

Muscovite was found only as a rare product of hydrothermal alteration in stockscheider and near the greisen stringers.

Topaz

Two types of topaz were encountered. Euhedral to subhedral equidimensional crystals with intensive oscillatory CL-zoning (Tp1) are enclosed in all rock types and topaz poses as one of the earliest crystallised minerals. Some large euhedral crystals contain zone-arranged quartz inclusions (Fig. 8a) and are strongly CL zoned. But no zoning in F or Si/Al ratio was observed.

Late, interstitial topaz (Tp2) occurs only in the dyke granite.

Both topaz types are rich in fluorine; nearly all F-OH sites are occupied by F. Only subtle differences were found between F contents of the stock granite (18.5–19.5 wt% F; i.e. 90–95% of theoretical F-saturation) and dyke granites (20–21 wt% F; 95–100% saturation).

Both Tp1 and Tp2 from the dyke granite are enriched in phosphorus, up to 0.5 wt% of P_2O_5. Some phosphorus enrichment in topaz was reported by London (1992) from fractionated granites in Cornubian pluton, but no quantitative data were yet published.

Phosphates

Two generations of fluorapatite were distinguished in all rock types: early Mn-poor euhedral crystals (Fig. 8b, and later Mn-rich interstitial flakes. Both types are poor in Cl (mostly below 0.1 wt% Cl) and show intensive yellow CL.

Amblygonite, childrenite-eosphorite, zwiesselite, and triphylite were found in the dyke granite. Their texture (small interstitial grains) suggests relatively late, but still magmatic origin (Table 6). Brown apatite forms small nests and aggregates with zinnwaldite in a layered zone immediately below the UST layer.

Tab. 5. Chemical composition (in wt%) and empirical formulae (based on 22 oxygen atoms per formula unit) of micas from Podlesí (boreholes PTP-1, PTP-3, quarry and outcrops). Content of Li, Rb, Cs and F was analysed from mica concentrates (more than 98% purity) using chemical methods, other elements in thin sections by EMPA (all in laboratory CGS Praha).

No.	3430	3434	3438	3445	3446	3452	3458	3464	3470	3492	3500	3510	2754	3359	3365	3385	3397	3416	3413
locality m	PTP-1 136	PTP-1 169	PTP-1 216	PTP-1 308	PTP-3 22	PTP-3 49	PTP-3 80	PTP-3 106	PTP-3 151	PTP-3 245	PTP-3 293	PTP-3 343	outcrop	outcrop	outcrop	outcrop	outcrop	quarry	quarry
rock type	dyke granite	stock granite	stock granite	stock granite	dyke granite	stock granite	stock granite	biotite granite	biotite granite	stock granite	stock granite	stock granite	upper stock granite	aplite dyke	biotite greisen	upper stock granite	upper dyke granite	laminated dyke granite	homogen dyke granite
SiO_2	47.61	45.08	42.02	43.16	45.89	45.94	46.48	43.82	36.99	44.20	45.94	44.41	47.66	44.35	38.38	41.54	47.76	49.29	49.02
TiO_2	0.21	0.48	0.71	0.54	0.28	0.29	0.25	0.56	1.72	0.28	0.34	0.67	0.38	0.39	0.10	0.57	0.20	0.12	0.20
Al_2O_3	19.78	20.57	21.31	21.42	20.42	20.35	20.16	20.50	17.84	20.23	20.46	20.65	20.51	20.63	22.35	20.40	19.57	19.88	20.05
FeO	11.15	13.58	16.25	15.48	12.56	13.50	12.30	14.94	22.77	13.60	12.87	14.06	12.25	13.82	20.20	17.43	10.76	10.50	8.60
MnO	0.25	0.08	0.17	0.08	0.19	0.05	0.11	0.10	0.21	0.14	0.15	0.11	0.04	0.05	0.07	0.53	0.13	0.25	0.02
MgO	0.25	0.52	0.73	0.56	0.21	0.26	0.39	0.42	1.57	0.39	0.31	0.34	0.38	0.32	0.26	0.10	0.35	0.04	0.45
Na_2O	0.51	0.52	0.53	0.45	0.46	0.45	0.46	0.50	0.59	0.53	0.53	0.47	0.52	0.45	0.25	0.48	0.58	0.57	0.23
K_2O	10.26	10.19	9.99	10.09	10.28	10.29	10.23	10.23	9.64	9.92	10.26	10.32	10.46	10.09	9.36	10.02	10.39	10.37	9.25
Rb_2O	1.071	1.064	0.860	0.720	1.080	1.038	1.083	1.002	0.841	1.103	1.043	0.915	0.893	0.786	0.571	0.675	0.698	1.031	1.216
Cs_2O	0.122	0.172	0.195	0.140	0.146	0.192	0.155	0.180	0.131	0.158	0.139	0.169	0.126	0.065	0.093	0.188	0.109	0.103	0.114
Li_2O	3.65	3.34	2.15	2.95	3.37	3.27	3.49	2.9	2.03	3.69	3.63	3.16	4.3	3.45	1.662	1.663	4.62	4.53	4.69
F	6.67	6.606	5.246	4.98	6.24	6.824	6.81	5.394	4.842	6.324	6.854	6.324	7.417	6.292	5.412	5.215	7.679	7.4	7.664
Total	**101.53**	**102.20**	**100.16**	**100.56**	**101.13**	**102.46**	**101.91**	**100.55**	**99.18**	**100.57**	**102.51**	**101.60**	**104.94**	**100.69**	**98.71**	**98.81**	**102.85**	**104.08**	**101.50**
2F=O	2.81	2.78	2.21	2.10	2.63	2.87	2.87	2.27	2.04	2.66	2.89	2.66	3.12	2.65	2.28	2.20	3.23	3.12	3.23
Σ	98.72	99.41	97.95	98.46	98.50	99.59	99.05	98.28	97.14	97.90	99.62	98.94	101.81	98.04	96.43	96.61	99.61	100.96	98.28
*Si	6.76	6.46	6.20	6.25	6.58	6.57	6.63	6.38	5.78	6.43	6.54	6.41	6.59	6.42	5.86	6.27	6.71	6.80	6.81
*Al	3.31	3.47	3.71	3.66	3.45	3.42	3.39	3.51	3.29	3.46	3.43	3.51	3.34	3.52	4.10	3.62	3.24	3.23	3.37
*Ti	0.02	0.05	0.08	0.06	0.03	0.03	0.02	0.06	0.20	0.03	0.04	0.07	0.04	0.04	0.01	0.07	0.02	0.01	0.02
*Fe	1.32	1.63	2.01	1.88	1.51	1.61	1.47	1.82	2.98	1.65	1.53	1.70	1.42	1.68	2.58	2.19	1.26	1.21	1.01
*Mg	0.04	0.11	0.16	0.12	0.05	0.06	0.08	0.09	0.36	0.09	0.06	0.07	0.08	0.07	0.03	0.01	0.04	0.01	0.06
*Mn	0.03	0.01	0.02	0.01	0.02	0.01	0.01	0.01	0.03	0.02	0.02	0.01	0.00	0.01	0.02	0.12	0.03	0.03	0.00
*Li	2.07	1.91	1.27	1.71	1.93	1.87	1.99	1.69	1.27	2.15	2.07	1.82	2.38	2.00	1.01	1.00	2.60	2.50	2.60
*K	1.86	1.86	1.88	1.86	1.88	1.88	1.86	1.90	1.92	1.84	1.86	1.90	1.84	1.86	1.83	1.92	1.86	1.82	1.66
*Na	0.14	0.14	0.15	0.13	0.13	0.13	0.13	0.14	0.18	0.15	0.15	0.13	0.14	0.13	0.08	0.15	0.16	0.15	0.07
*Rb	0.10	0.10	0.08	0.07	0.10	0.10	0.10	0.10	0.09	0.11	0.10	0.09	0.08	0.08	0.06	0.07	0.07	0.09	0.11
*Cs	0.01	0.01	0.01	0.01	0.01	0.01	0.01	0.01	0.01	0.01	0.01	0.01	0.01	0.00	0.01	0.01	0.01	0.01	0.01
*F	2.99	2.99	2.44	2.28	2.83	3.08	3.07	2.48	2.39	2.91	3.08	2.88	3.24	2.88	2.61	2.48	3.41	3.22	3.36

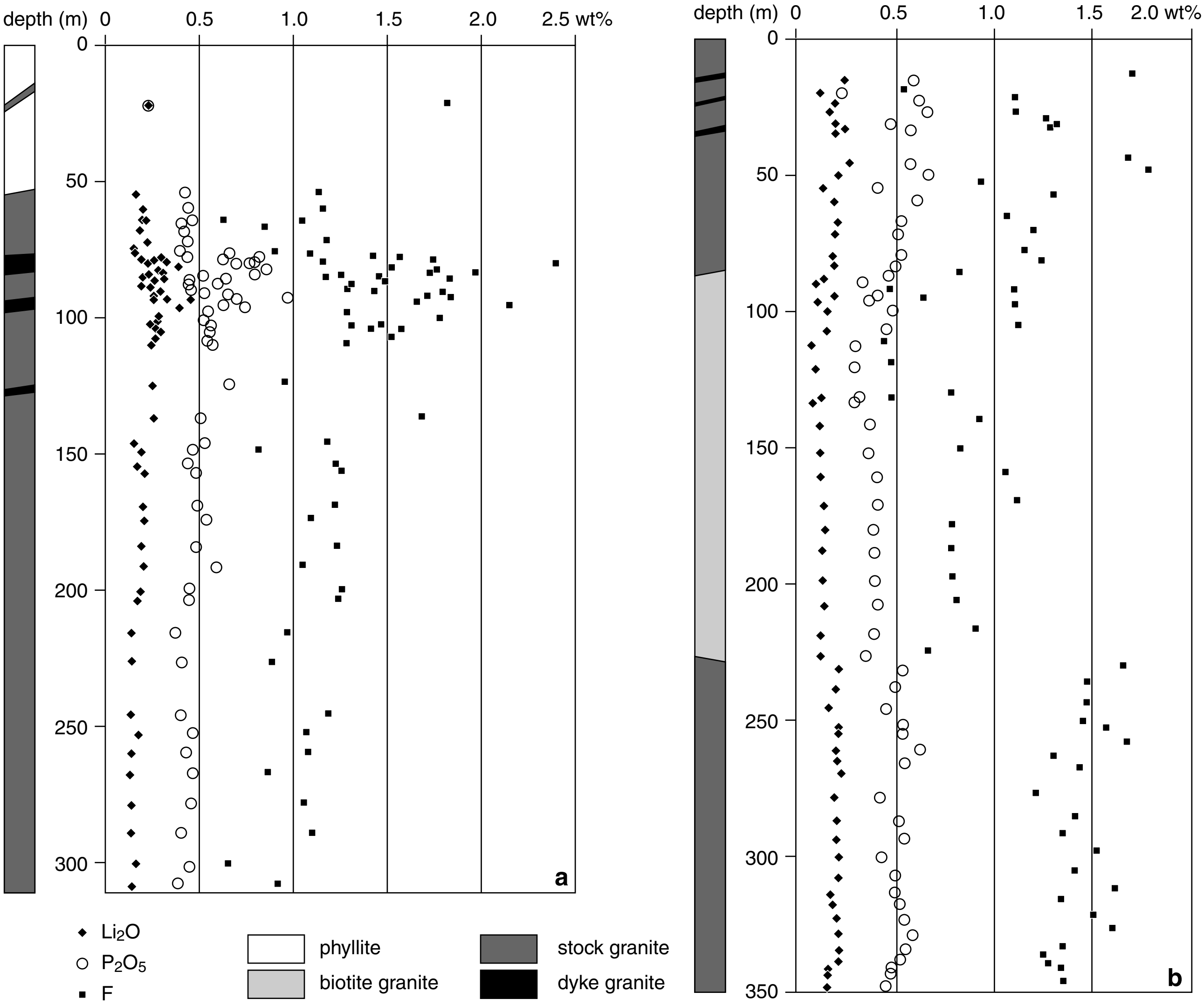

Fig. 11. Contents of chemical elements in boreholes: a – borehole PTP-1, b – borehole PTP-3.

Small nests (up to 1 mm^2) of late amblygonite and hydrated phosphates of Al, Ca, Fe and Mn were also identified in the dyke granite. Among them, only morinite has been clearly identified. Some of the late phosphates appear to have concentrated strontium during a hydrothermal stage. Sr contents reach max. 1 wt%. According to Kostitsyn and Breiter (2001), this mobile strontium was largely of radiogenic origin.

Tourmaline

Tourmaline is rare in all granite types. Black tourmaline of schorl type (blue-brown under crossed polars) fills small pockets in UST layers within the dyke granite and seems to be primary late magmatic. Black tourmaline (blue under crossed polars) of probably metasomatic origin occurs together with secondary quartz in globular aggregates up to 5 cm across in deeper part of the stock granite.

Other accessories

Small euhedral monazite crystals occur mainly as inclusions in micas, in some places surrounded by pleochroic halos. Monazite is the main Th and REE host in all rock types, and is replaced by abundant brabantite in the dyke granite (Förster 2001). The most important carrier of U is Th-poor uraninite. Zircon is scarce in both granite types (Förster 2001); the habit of crystals is dominantly the combination of (110) and (101) (P. Uher, pers. comm.).

Nb-Ta oxides are the most abundant oxide minerals (Fig.14). Small grains of Nb- and Ta-rich rutile are common in all rock types. They occur mainly as inclusions in mica flakes, in places forming zonally arranged clusters in their core areas. Columbite, present only in the dyke granite, is partly included in micas, and partly interstitial. Ta-rich rutile occurs mainly in the pegmatite-like UST layers.

The stock granite also contains accessory amounts of wolframite, cassiterite, pyrite, bismuthine and molybden-

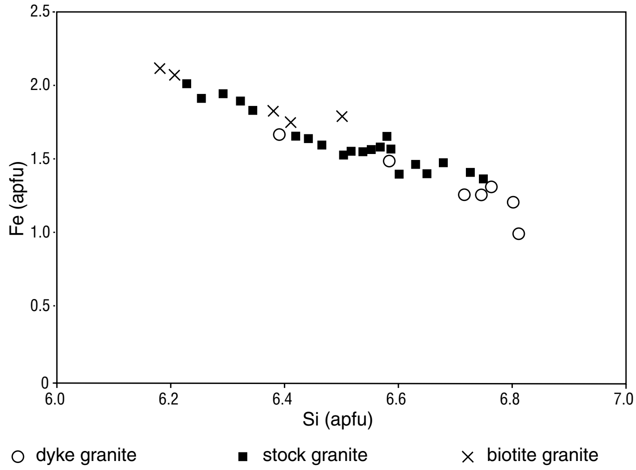

Fig. 12. Classification of micas in Si-Fe plot in atoms per formula unit (apfu). Zinnwaldites are depleted in Fe in comparison with protolithionites and lithian biotites. The micas with Fe apfu >2 can be classified as Li-biotite, micas with 2 > Fe apfu > 1.5 as protolithionite and micas with Fe apfu <1.5 are zinnwaldites.

ite. Other accessory minerals present in the dyke granite include cassiterite, hematite, pyrite, bismuthine, scheelite, ixiolite, U-microlite and U-tantalite.

Discussion

Geological features

The Podlesí stock is not the only outcrop of P- and F-rich granite in the area of Horní Blatná. Similar rocks outcrop at the southern margin of the Horní Blatná body (small stock NE of the village of Pernink) and was also found in drill core of the Uranium industry enterprise on the NE margin of the Horní Blatná body (borehole JD-64) – see Breiter et al. (1987). Several dm thick dyke, very similar in composition to the Podlesí stock granite, cuts the biotite granite of the Horní Blatná body about 2 km to the south from the Podlesí stock. The time interval between the emplacement (s) of the Horní Blatná body and the Podlesí stock is about 1–5 Ma (unpublished Ar/Ar data by S. Scharbert). It seems probable that the Horní Blatná body and the Podlesí stock are products of fractionation of the same source. Nevertheless, a chemical gap exists between the biotite granites of the Horní Blatná body and P- and F-rich Li-mica granites of Podlesí.

Origin of specialised melts

The Podlesí stock as a whole is strongly enriched in lithophile elements F, P, Li, Rb, Cs, U and rare metals Sn, Nb, Ta and W. Individual most-evolved domains within the system are extremely enriched in some of these elements. According to all petrological observations, the extreme geochemical specialisation within the system is magmatic. The origin of such highly fractionated and specialised melt can be explained in several steps:

1. Origin of P-enriched stock granite melt (“parental melt” of the Podlesí system) from the “common” melt of the younger intrusive complex (YIC) of the Nejdek-Eibenstock pluton: the YIC itself represents a relatively strongly fractionated suite with late members rich in F, Li, Rb, Sn and also P. Although a chemical gap exists between the late YIC granites from the northern part of the Horní Blatná body (Breiter et al. 1987) and the stock granite from Podlesí, a genetic link between these rocks is possible and highly probable. The extreme enrichment in phosphorus during the fractionation was due to a combination of low content of calcium and high peraluminosity of the YIC melt. High peraluminosity suppressed the nucleation of apatite, all Ca was incorporated in early plagioclase, and P was retained in residual melt. No special P-rich protolith was needed (Breiter 1998).
2. The origin of the dyke granite melt (“residual melt”): continued fractionation of the stock granite melt during the emplacement, and also after the emplacement (in a deeper part of the system), produced small domains of residual water-rich melt even more strongly enriched in P, F, Li, Rb, Nb, Ta, W, U etc. High contents of depolymerising cations in residual melt caused their lower viscosity and higher mobility (Mysen 1987).

Tab. 6. Chemical composition (in wt%) and empirical formulae of phosphates from Podlesí (analysed by EMPA in laboratory CGS Praha).

Sample	2360	2669	2669	2651	2651	2651
Mineral	Amblygonite	Childrenite	Eosphorite	Zwieselite	Triplite	Morinite
Na_2O	4.24			0.02		4.27
CaO				2.1	0.55	13.77
FeO	0.42	20.61	9.74	34.36	19.77	3.65
MnO		11.02	21.74	22.81	38.56	6.43
MgO				0.24	1	1.61
Al_2O_3	34.81	22.17	21.35		0.03	20.28
TiO_2	0.42			0.23	0.08	
P_2O_5	45.6	31.41	31.54	31.59	31.48	29.52
F				5.41	5.03	12.77
TOTAL	95.85	85.2	84.37	96.88	96.5	92.39
Na						0.05
Ca				0.09	0.02	1.18
Fe		0.65	0.31	1.11	0.63	0.24
Mn		0.35	0.7	0.75	1.25	0.44
Mg				0.02	0.06	0.19
Al	1.01	0.99	0.96			1.99
Ti	0.01			0.01		
P	0.95	1.01	1.02	1.03	1.02	2
F				0.57	0.53	2.79
O	4	5	5	4.5	4.5	10.5
Fe/(Fe+Mn)		0.65	0.31		0.6	0.34

This "melt" was a mixture of water-rich silicate liquid and entrained quartz, feldspars, mica and topaz crystals. Individual bubbles of residual melt coalesced and intruded upward.

3. *In situ* fractionation within the major dyke: in spite of the high content of crystals, the melt contained enough water, fluorine, phosphorus and lithium for fractionation to continue. Under such conditions, the crystallisation would have started from the lower dyke contact and proceeded upward (Morgan and London 1999).

Zoning of main rock-forming minerals

Zoning of Kfs and mica from the dyke granite gives evidence for two major stages in the crystallisation history of this rock, whereas only one major crystallisation stage was observed within the stock granite. The unzoned Kfs and mica crystals from the stock granite are nearly identical with the Kfs cores and mica cores from the dyke granite and represent the older crystallisation stage from the "parental" melt. In contrast, the P-enriched rims of Kfs and Li-enriched rims of mica found only in the dyke granite document a distinctly more evolved environment enriched in phosphorus and fluorine, i.e. the "residual" melt.

P-rich rims on Kfs and albite provide evidence for a magmatic origin of all feldspars. As the distribution coefficient of phosphorus between melt and fluid is higher than 1 (London et al. 1993), the melt should be richer in P than the coexisting fluids. Thus, the P-rich rims of Kfs and some albites in the dyke granite argue for principally magmatic crystallisation of the rocks from an evolved residual melt without any later P redistribution (Frýda and Breiter 1995).

High fluorine saturation

The entire Podlesí stock is rich in fluorine. The stock granite contains 0.6–1.8 wt% F and the dyke granite contains 1.4–2.4 wt% fluorine. F content of residual crystallised melt should be even higher. High content of F in amblygonite (9.4–10.3 wt%) reflects, according to London et al. (2001), 2.5–3.0 wt% of fluorine in crystallised melts. This is consistent also with the contents of fluorine in zinnwaldite and topaz, which are higher than 90% of theoretical maximum in both minerals from the dyke granite.

Boron saturation

The present content of B in the rock is negligible at 20–60 ppm, but an extensive exo-contact aureole of tourmalinisation in phyllite indicates a large supply of boron must have emanated from the crystallised magma. Crystallisation of tourmaline in equilibrium with Fe-mica in relevant conditions (500–600 °C, 1 kbar) requires about 2% of B in the melt. High content of fluorine requires even higher contents of B at this equilibrium (Wolf and London 1997). Although no primary magmatic tourmaline was found in granite, the primary boron content in melt probably did not exceed 2–2.5%. The only exception are small pockets within the UST layers up to 4 mm in diameter and filled by tourmaline. Here, droplets of residual liquids likely crystallised far from equilibrium conditions.

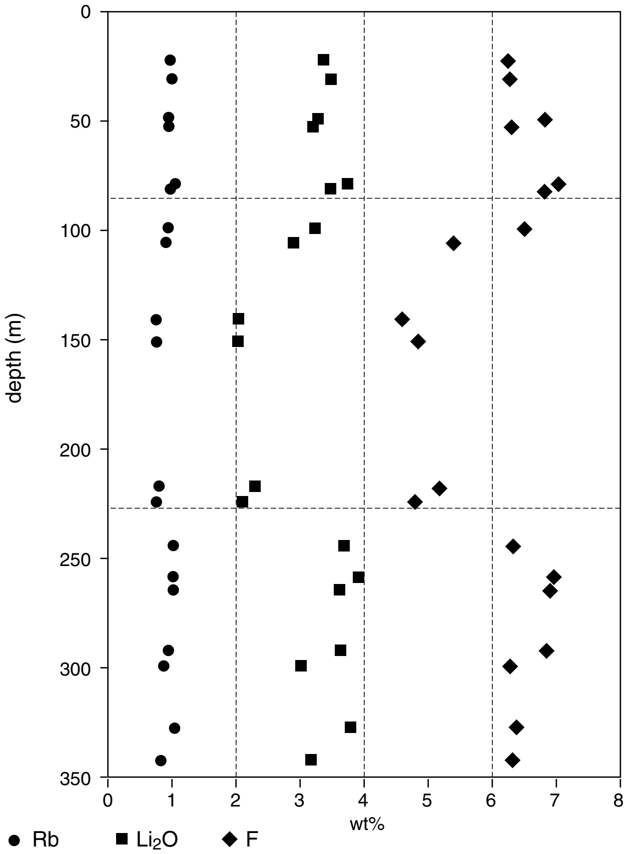

Fig. 13. Contents of Rb, Li_2O and F (wt%) in micas along the borehole PTP-3. The contacts between the upper and the lower body of the stock granite and the biotite granite in the middle are also marked. The contents of Rb are rather similar along the whole profile. In contrast, the Li_2O- and F-contents are sensitive indicators of granite types.

The rounded tourmaline-quartz aggregates ("tourmaline suns") found in deeper parts of the stock granite and in the enclosing biotite granite are hydrothermal in origin.

Explosive breccia with granitic matrix

Although magmatic breccias are a common feature associated with shallow-level intrusions of rare-metal granites in the Krušné hory/Erzgebirge and Slavkovský Les area (Krupka, Krásno, Seifen, Sadisdorf, Gottesberg) and elsewhere (Cornwall), recognition of their real significance is relatively young (Oelsner 1952, Schust and Wasternack 1962, Allman-Ward et al. 1982, Seltmann and Schilka 1991, Jarchovský and Pavlů 1991). At Krupka, for example, a spectacular chimney-like body of gneissic breccia cemented by Mo- and W-bearing greisen was formerly described as tectonic breccia (Beck 1914) and only much later was its magmatic origin uncovered (Eisenreich

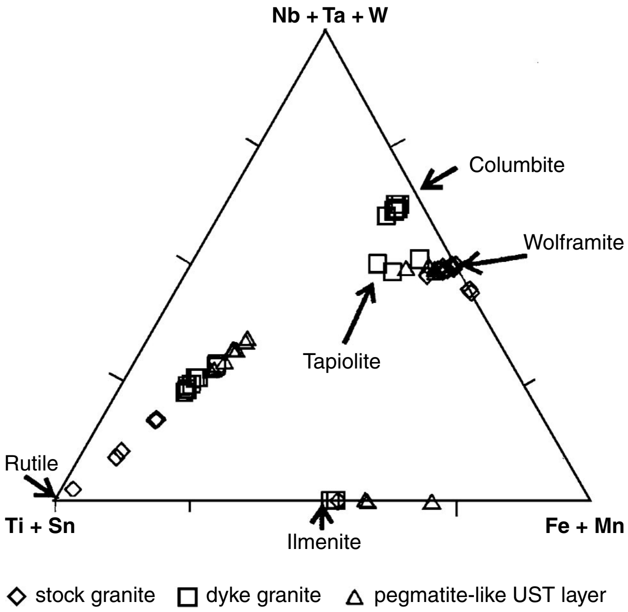

Fig. 14. Classification of Nb-Ta minerals.

and Breiter 1993). In Krušné hory Mts., both geochemical types of ore-bearing granites produced brecciation, the slightly peraluminous P-poor granites (Krupka, Sadisdorf, Gottesberg, Seifen) as well as the strongly peraluminous P-rich granites (Krásno).

The Podlesí granite is no exception in the family of Krušné hory/Erzgebirge ore-bearing granites; here, proof of magmatic brecciation is evident in an individual block of breccia that was found near the upper contact of the stock (Fig. 5a). Original shape of the breccia body can't be reconstructed now. The breccia comprises phyllite fragments (5–50 mm across) supported by fine-grained granite matrix. Although the matrix has mineralogical composition similar to the stock granite, its origin should be connected with the emplacement of the first portion of the stock granite melt. Genetic interpretation of the breccia is rather speculative; 1. the breccia was found only at the hangingwall-contact of the stock, where the volatile components reached during intrusion its maximal concentration, 2. at the same time, no hydrothermal overprint was found neither in clasts, nor in matrix. Therefore, we have found the explosive nature of this breccia most probable.

Layering in parts of the stock, in stock granite and in the major dyke, indicates episodic opening of the system occurred, possibly accompanied by brecciation. Other evidence of brecciation is represented by the thin veinlets in crystals of quartz (Fig. 8h) and feldspars filled with residual, extremely specialised magmatic liquid. Sudden decrease of pressure caused decrepitating of larger crystals within the newly crystallised dyke. Residual liquids were drawn from interstices into opened cracks in crystals and rapidly crystallised. Just as the layered upper part of the major dyke crystallised in non-equilibrium conditions, so also did the isolated droplets of residual liquids, which are of very different composition. Although it is impossible to obtain representative chemical analyses of these veinlets, at least two different types are recognised, one Na+F-rich (Q+Ab+Tp) and the other K+P-rich (Kfs+Ap). This fits well with two types of melt inclusions in quartz from the dyke granite found by Thomas (Breiter et al. 1997).

Origin of flat dykes

Dominantly flat orientations of dyke granite were found in outcrops and boreholes. The only steep dykes have been encountered in the uppermost parts of the boreholes PTP-1 and PTP-4 with max. thickness about 5–20 cm. No expected feeder zones have been found in the deeper part of the stock. Several models for the origin of the dykes were postulated during the last three decades: intrusive (Komárek 1968), metasomatic (Lhotský et al. 1987), and filter-pressing (Breiter and Seltmann 1995). The metasomatic origin explained via "greisenisation" was ruled out when the two-stage magmatic evolution of feldspars and micas was recognised (Breiter et al. 1997). Recent finds of layering and USTs argue for intrusion of the whole batch of dyke-granite melt into opened structure and subsequent "*in situ*" fractionation.

Magmatic layering and USTs

Simple magmatic layering with non-oriented crystallisation or with orientation of minerals parallel to the layers is relatively common in aplite-pegmatite bodies. In such bodies, layers enriched in quartz alternate with layers enriched in albite, K-feldspar, garnet or tourmaline (Breaks and Moore 1992, Morgan and London 1999). Generally, such type of layering evolved near the footwall of flat pegmatite-aplite bodies and crystallised upward (Tanco, Little Three etc.). The largest well-described example of magmatic layering is the Calamity Peak granite-pegmatite complex in South Dakota, USA. This boron-rich pluton includes about 400 m thick complex of alternating pegmatite and layered aplite, in layers 0.1–2 m thick (Duke et al. 1992).

Magmatic layering in true granites is less abundant. When it occurs, it has generally evolved near the roof of the intrusion and crystallised downward (Baluj 1995, Zarajsky et al. 1997).

Magmatic layering with crystals oriented perpendicular to the individual layers (now termed UST) typically evolved in subvolcanic granitic stocks associated with Mo, W ± Sn mineralisation. Layering is typically parallel to the contact and is expressed by alternation of layers composed of euhedral quartz crystals and layers of fine-grained aplite. This remarkable feature was described under different terms from Transbaykalia and Kazakhstan a long time ago (Kormilitsyn and Manuilova 1957, Povilaytis 1961), but, published only in Russian, it did not attract attention. Later, Shannon et al. (1982) introduced this phenomenon into English-speaking geological community. These authors also coined the non-genetic (primarily metallurgic) term "unidirectional solidification texture" (UST), also used in this article. Several years later, Kirkham and Sinclair (1988) introduced the term "comb quartz layers" for specific type of UST with predominance of quartz crystals.

Besides Mo-bearing porphyries, USTs have been described also from pegmatite-aplites (London 1992). Unlike in the porphyries, USTs in aplite-pegmatites are expressed not only by quartz, but also by K-feldspar. Duke et al. (1992) reported perthite and tourmaline crystals growing approximately normally to the contact planes of pegmatite layers in the Calamity Peak pluton, South Dakota. This feature is abundant near the upper contact, but was also found at the footwall contact indicating crystallisation inward from both contacts. Webber et al. (1997) reported quartz and tourmaline crystallised perpendicular to the layering from the GAB pegmatite-aplite dyke, California. Stephenson (1990) described UST with comb quartz and quartz-Kfs myrmekitic fan-like aggregates from a hypersolvus granite of East pluton in Hinchinbrook Island, Australia.

In layered granites, the bulk composition of layered parts of the magmatic body is similar to the bulk composition of the whole body (Zarajsky et al. 1997). The layered aplite-pegmatites are often differentiated into slightly Na-enriched lower aplite and K-enriched upper pegmatite (Duke et al. 1992, Breaks and Moore 1992, Morgan and London 1999). In contrast, UST rocks in porphyry-type systems (comb quartz + interstitial aplite) may contain 60% modal quartz or more; consequently, the bulk compositions do not represent magmatic compositions of the whole bodies and thus are not consistent with the overall granitic composition of parental porphyry melt. The intensive silica enrichment within the comb layers was explained by models based on open-system addition of quartz crystallising from aqueous fluid. This fluid is thought to have separated from the magma column by resurgent boiling (Kirkham and Sinclair 1988) or by convective degassing (Lowenstern and Sinclair 1996).

McBirney and Noyes (1979) proposed the oscillatory supersaturation of a boundary layer on crystallisation front as a main feature for rhythmical layering in basic rocks. Layering in more acid systems, although studied intensively in last decades, was still not explained satisfactorily (see overview in London 1992). Models for layering in granitic rocks based on experimental work have been developed recently. Webber et al. (1997) stressed the significance of undercooling for heterogeneous nucleation and oscillatory crystal growth in aplite-pegmatite systems. London (1999), based on experiments with B, F, P-dotted granitic melt, preferred the boundary-layer effect in undercooled melt (>100 °C below the liquidus) as sufficient base for evolution of layered textures. Balashov et al. (2000) developed a model of "swinging eutectic" for the albite-quartz and albite-K-feldspar systems. The oscillation of fluid pressure (due to episodic melt degassing) resulted in expanding of either the quartz field at high pressure or the albite field at low pressure and further crystallisation of albite-quartz line rock. Fedkin et al. (2002) made experiments with P- and F-doted common granite and geochemicaly evolved granite from Podlesí. The runs with evolved granite-melt produced line rock as rhythmically alternated thin bands in the upper part of the experimental glass specimen. The alternating bands exhibit differences in the content of Al, Si, F, P and alkalis.

At Podlesí, individual UST layers reached a maximum thickness of 1 m (borehole PTP-1, depth 86–87 m). The well-documented UST layer of the major dyke exposed in the old quarry is about 40–45 cm thick. Comb quartz crystals are only subordinately developed here in the upper laminated half of the UST sequence. The most significant UST layer is defined by Kfs. This mineralogical feature, and also the bulk chemistry with strong enrichment of LILE, make the Podlesí system more comparable with UST layers in aplite-pegmatite bodies than with those from porphyry intrusions. Nevertheless, with the exception of 10 cm thick Kfs-dominated UST, there is no K-enrichment and Na-depletion in the upper part of the dyke.

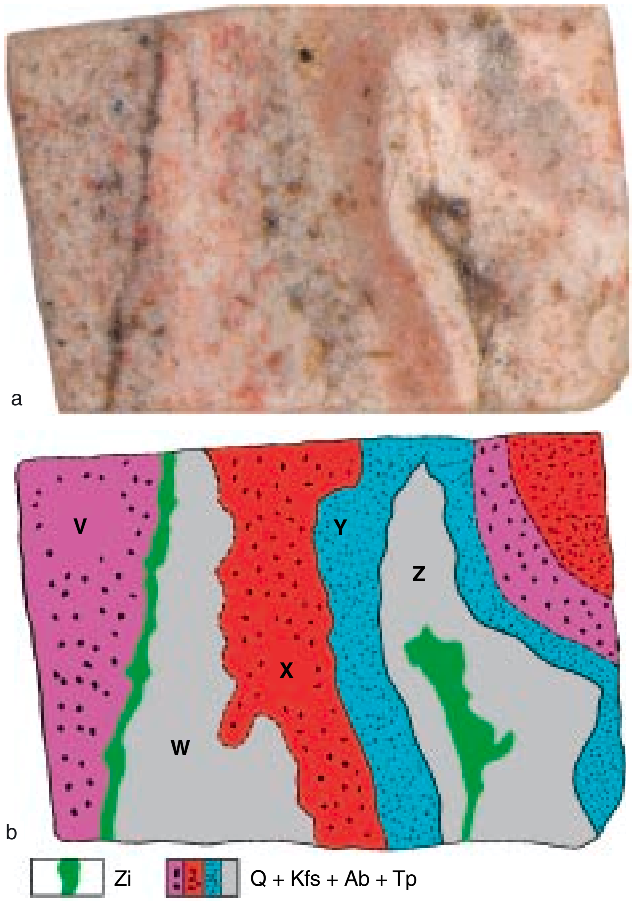

Fig. 15. A detail of the folded laminated dyke granite (sample 3402b): a – photo, b – schema of analysed domains (compare Table 4). Area of the image is 30 × 20 mm. Abbreviations: Zi – zinnwaldite, Q – quartz, Kfs – K-feldspar, Ab – albite, Tp – topaz.

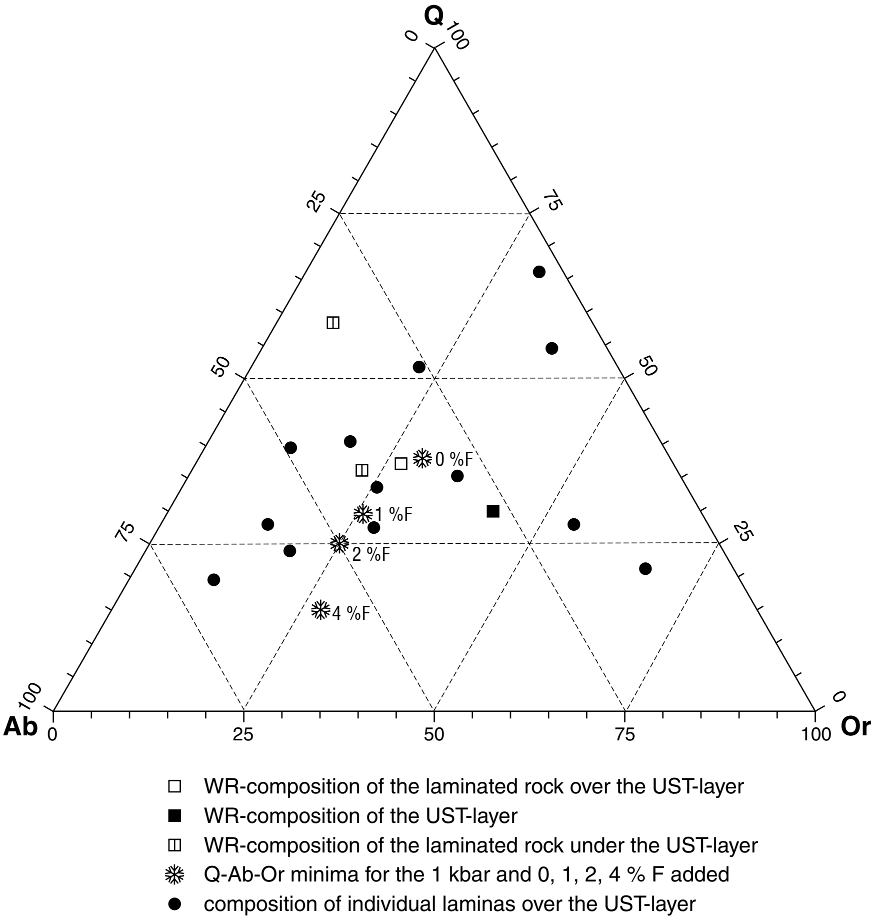

Fig. 16. Q-Ab-Or triangle for laminated rocks. The WR-analyse of this area is No. *3416* in Table 1. The position of the minima for the water-saturated system without F and with added 1, 2, 4 wt% F (p_{H2O} =1 kbar) (Manning 1981) are also indicated.

The chemical bulk composition of the upper laminated part of layered sequence of the major dyke (anal. 3416 in Table 1) with small individual comb quartz layers (4–5 mm) is similar to the bulk composition of the whole dyke. Nevertheless, the bulk composition of the K-feldspar-dominated UST layer (anal. 3417 in Table 1) is far from the bulk composition of the dyke granite melt; instead, it is strongly enriched in K and Al and depleted in Si and Na. The bulk composition of the UST layer can be modelled as a mixture of the dyke-granite melt with 25% of Kfs added. This means that another Kfs component was added to the granitic Q-Ab-Kfs matrix. At this point, it would be interesting to compare the Kfs-dominated UST layer with the stockscheider, which also contains many large Kfs crystals; the bulk composition of the stockscheider (anal. 3361 in Table1) is equal to the bulk composition of the stock granite. Consequently, the large Kfs crystals in the stockscheider are well compensated by quartz-albite matrix, and no addition of Kfs or potassium has occurred. Another difference between the Kfs-rich UST and the stockscheider lies in the contents of volatiles and LILE: the stockscheider is poor in P, F, Li and Rb compared to the stock granite. In contrast, the Kfs-rich UST is enriched in Rb, Li and Cs compared to the overall composition of the dyke granite. It can be deduced that, in the case of the stockscheider, the mobile alkalis partitioned into aqueous fluids and escaped into the exocontact zone, whereas in case of UST all these elements were incorporated into the crystallised Kfs and zinnwaldite. In case of F and P, where are large melt/vapor partition coefficients, it will be necessary to find another mechanism of depletion in the stockschneider.

The change of the isotropic granitic fabric of the uppermost laminated layer of the major dyke to anisotropic fabric of the UST layer reflects a change from equilibrium crystallisation of the granitic layer to disequilibrium crystallisation of the UST layer. The disequilibrium was caused especially by undercooling. The growth of large comb Kfs crystals was facilitated by combined enrichment in fluorine, phosphorus and water. All these components increased the ability of the melt to be undercooled, suppressed the nucleation density and made the lag time longer (slower crystallisation response of volatile-bearing melt to cooling, London 1996). As a result, the residual melt of the dyke granite was able to survive undercooling well below 500 °C.

Fenn (1977) stated that nucleation density of feldspar fell sharply with increasing H_2O, which resulted in the growth of large crystals from H_2O-saturated melt. In the same grade of undercooling, the nucleation density of Afs is suppressed much more than that of quartz (London et al. 1989), so the Kfs are larger than the associated quartz.

Rapid growth of large Kfs promoted local saturation of non-consumed constituents of the melt at the margin of the growth front. This resulted in the crystallisation of small albite crystals zonally arranged in outer parts of comb Kfs (Fig. 8c). This is the same process as the origin of the so-called snowball quartz (Schwarz 1991) (Fig. 8e).

The newly crystallised fine-grained layers were not entirely solid while interstitial melt was still present. As a consequence, individual layers were ptygmatically deformed in many places (Fig. 6, 15). Minute, cm-scale intrusions of residual melt into older layers also occurred (Fig. 8g).

Mineralogical and chemical composition and grain size of individual laminae differ significantly (Table 4, Fig. 15). Boundaries between laminae are commonly sharp (Fig. 8f), but in places diffuse (Fig. 7c). The large scatter of normative compositions of individual laminae relative to F-enriched granite minima (Fig. 16) reflect non-equilibrium crystallisation in open system.

Substantial difference between the majority of mentioned models and the Podlesí granite systems is in the content of boron. Calamity Peak layered system contains 0.3–0.5 wt% of B_2O_3 (Duke et al. 1992). London (1999) used for his experiments haplogranite dotted by 2.9 wt% of B_2O_3. The actual content of boron in Podlesí rocks is negligible (<60 ppm). In spite of that, undercooling may be considered as the crucial factor triggered the evolution of magmatic layering and UST also in case of Podlesí. Large scatter of quartz-feldspars ratio within the laminated dyke (Fig. 16) indicates, that also the model of "swinging eutectic" (Balashov et al. 2000) should be taken into account.

The evolution of the major dyke at Podlesí should be generally explained in agreement with models by Webber (1997) and London (1999) for layered aplite-pegmatite bodies: The crystallisation started in the footwall and produced equigranular fine-grained albite-zinnwaldite-topaz granite. Concentration of water in the upper, not yet crystallised, part of the melt and its subsequent exsolution ("second boiling") caused overpressure and resulted in rupturing of overlying rocks and sudden opening of the system. Adiabatic cooling due to the escape of water and other volatiles caused undercooling of melt. Repeated opening/closing of the system produced inhomogeneities in the upper part of the major dyke resulting in crystallisation of line rocks with thin chemically contrasting laminae. This crystallisation started in the hangingwall and continued downwards. Undercooling made the lag time longer and the density of nucleation lower. This promoted the UST-style of crystallisation (according to the model introduced for pegmatites by London 1992, 1996). There is no evidence yet of a "meeting point" of the footwall- and the hangingwall-started crystallisation. During episodic opening of the system, droplets of extremely enriched residual liquids, so far entrapped in rock pores, were also liberated and filled newly opened cracks in minerals. Two types of melt inclusions in quartz – one F-rich and another P-rich – have been documented by Thomas (in Breiter et al. 1997a). These correspond well to topaz-rich and apatite-rich veinlets that cut quartz and Kfs crystals near the upper dyke contact.

Reaction between granite and aqueous fluid

Aqueous fluid-related processes developed within the granite stock only locally. F-rich, Li-poor fluids caused greisenisation of all granite types, and P-rich fluids supported crystallisation of late phosphates within the layered domains of the dyke granite. At this stage, Sr was partially mobilised and incorporated into late phosphates.

Escape of aqueous phase

Icenhower and London (1996) found $D_{Rb}^{Kfs/melt} = 1$ for geologically relevant conditions. At Podlesí, the actual contents of Rb in Kfs are distinctly higher than should be expected from the whole-rock data. Thomas (in Breiter et al. 1997) reported high Rb values (0.6–0.7 wt% Rb_2O) in crystallising melt based on the composition of melt inclusions in quartz. The crystallised melt was thus much more rich in Rb than the actual granite.

An extensive 100–200 m thick aureole of tourmalinisation and Rb enrichment up to 400 ppm compared to regional values of 250 ppm was detected within the phyllite enveloping the Podlesí stock (Breiter, unpublished data). This argues for release of aqueous fluids from the crystallised granite body causing external metasomatism of the surrounding rocks. Nevertheless, distinguishing between the influence of the older, but more voluminous biotite granite pluton and the influence of volatile-enriched, but much smaller Podlesí stock, is not possible.

Conclusions

Taking account of all the above-discussed constraints for genetic interpretation, the following model is proposed:

– The whole evolution was generally magmatic, melt-related. Post-magmatic, aqueous phase-related processes were very restricted.
– Pronounced fractionation of the YIC melt produced a small amount of residual F, P, Li-rich melt (stock granite melt) which intruded as a tongue-like body into a "shallow depth". Emplacement of this body was accompanied by brecciation of the overlying phyllite. Composition of the emplaced "primary" melt was similar to that of the present stock granite. Its crystallisation started in the outer upper part of the stock. This represents the rapidly cooled primary melt without major late- and post-magmatic alteration. Fluids and volatiles were concentrated beneath the rapidly crystallised carapace.
– Subsequent fractionation in deeper parts of the stock produced a small amount of residual melt extremely enriched in F, P, Li and water. When the upper part of the stock had crystallised and cooled sufficiently to allow opening of brittle structures, this residual melt penetrated upward forming a set of flat dykes.
– The emplaced residual melt entrapped some grains of quartz, feldspar and mica inherited from the parental melt. Rims of these grains crystallised during ascent or *in situ* within the dykes.
– Crystallisation of the major dyke started in closed-system conditions from the bottom upwards. Volatiles migrated to the uppermost part of the dyke. After the pressure of exsolved water overcame the lithostathic

pressure and cohesion of surrounding rocks, the system opened. Propagation of existing cracks or opening of new cracks started. The fluid escaped and the sudden adiabatic decrease in pressure rapidly decreased temperature. The UST-rich layers crystallised from undercooled melt. This process might be repeated several times. Nonequilibrium crystallisation in layered rock produced small domains with contrasting chemistry and finally very small amount of liquids of unusual composition.

– High content of aqueous phase in the uppermost dyke of the "dyke granite" locally caused intensive greisenisation of this dyke (quartz+zinnwaldite greisen).
– Even later, during final consolidation of deeper parts of the system, F-rich and Li-poor aqueous phase were released. Aqueous phase, enriched in F, Li, Rb and Sn, ascended upwards along steep joints causing small-scale greisenisation (quartz+biotite±apatite greisens).

Acknowledgement. This work has been performed within the state scientific program "Complex geochemical research of interaction and migration of organic and inorganic chemicals in rock environment" supported by the Ministry of the Environment of the Czech Republic by grant project No. VaV/3/630/00.

I thank many colleagues who supported my investigation of the Podlesí granite system for years, ordered alphabetically: P. Dobeš, M. Eisenreich, H.-J. Förster, M. Chlupáčová, T. Jarchovský, F. Koller, Ju. Kostitsyn, J. Leichmann, P. Lhotský, A. Müller, P. Ondruš, T. Pačes, L. Raimbault, S. Scharbert, R. Seltmann, Š. Táborská, R. Thomas, P. Uher, F. Veselovský, K. Žák. My special thanks are addressed to J. Frýda and I. Vavřín for huge amount of microprobe analyses and to the staff of the chemical laboratory of the CGS (leaders V. Sixta and H. Vitková) for numerous whole-rock analyses.

Constructive reviews by T. Jarchovský, D. London and W. D. Sinclair helped to improve the manuscript significantly.

References

Allman-Ward P. et al. (1982): An Intrusive Hydrothermal Breccia Body at Wheal Remfry in the Western Part of the St. Austel Granite Pluton, Cornwall, England. In: Evans A.M. (ed) Metallization Associated with Acid Magmatism. 1–28. J. Wiley.

Balashov V. N., Zaraisky G. P., Seltmann R. (2000): Fluid-Magma Interaction and Oscillatory Phenomena during Crystallization of Granitic Melt by Accumulation and Escape of Water and Fluorine. Petrology, 8, 505–524.

Baluj G. A. (1995): Unique example of layered granitic melts in intrusions in the Coast Zone of the Primorie region. Doklady Akad. Nauk 341, 83–88. (in Russian).

Beck (1914): Die Zinnerzlagerstätten von Graupen in Böhmen. Jahrb. Geol. Reichsanstalt 64, 296–306.

Breaks F. W., Moore J. M. jr. (1992): The Ghost lake batholith, Superior province of northwestern Ontario: A fertile, S-type, peraluminous granite – rare element pegmatite system. Canadian Mineralogist 30, 835–875.

Breiter K. (2001a): Podlesí – the story of material and structural evolution of fluorine- and phosphorus-rich granite magma. Tektonik und Magma 2001, Workshop vom 22.–24.06.2001 in Bautzen.

Breiter K. (2001b, ed.): International Workshop Phosphorus- and Fluorine-rich fractionated granites, Podlesí. Abstracts, Excursion Guide, Programme. 108 p. Czech Geol. Surv., Praha.

Breiter K., Chlupáč I., Jarchovský T., Matějka D., Novák J. K., Štemprok M., Koller F., Göd R., Klötzli U. S., Slapansky P., Scharbert S., Seltmann R., Förster H.-J., Gottesmann B., Sala M., Wolf D., Müller A. (1998): Genetic significance of phosphorus in fractionated granites. Excursion guide. 170 p. Czech Geol. Surv., Praha.

Breiter K., Förster H.-J., Seltmann R. (1999): Variscan silicic magmatism and related tin-tungsten mineralization in the Erzgebirge-Slavkovský les metallogenic province. Mineralium Deposita 34, 505–521.

Breiter K., Frýda J. (2001): Phosphorus and rubidium in alkali feldspars – tools for better understanding of the late- to post-magmatic evolution of fractionated granites. In: A. Piestrzyński et al. (eds.) Mineral Deposits at the Beginning of the 21st Century. 393–396. Balkema Publishers, Lisse.

Breiter K., Frýda J., Leichmann J. (2002): Phosphorus and rubidium in alkali feldspars: Case studies and possible genetic interpretation. Bull. Czech Geol. Surv., 77, 2, 93–104.

Breiter K., Frýda J., Seltmann R., Thomas R. (1997a): Mineralogical evidence for two magmatic stages in the evolution of an extremely fractionated P-rich rare-metal granite: the Podlesí stock, Krušné hory, Czech Republic. J. Petrology 38, 12, 1723–1739.

Breiter K., Haková M., Sokol A. (1987): Geochemical types of granites in the Blatná massif in the Krušné hory Mts. Věst. Ústř. Úst. geol. 62, 333—349. (in Czech)

Breiter K., Knotek M., Pokorný L. (1991a): The Nejdek granite massif. Folia Mus. Rer. Nat. Boh. Occid., Geol. 25. 59 p. Plzeň.

Breiter K., Seltmann R. (1995, eds.): Ore mineralizations of the Krušné hory Mts. (Erzgebirge). – SGA Excursion Guide, Third Biennal SGA Meeting, Prague, 28–31 August 1995, Czech Geol. Surv. Prague, 205 p.

Breiter K., Seltmann R., Thomas R. (1997b): The phosphorus-rich rare metal granite system of Podlesí, Czech Republic. Proceedings of the fourth biennial SGA meeting, Turku/ Finland; ed. H. Papunen, A. A. Balkema. 833–835.

Breiter K., Sokolová M., Sokol A. (1991b): Geochemical specialization of the tin-bearing granitoid massifs of NW Bohemia. Mineralium Deposita 26, 298–606.

Chlupáčová M., Breiter K. (1998): Physical properties of extremely fractionated P-rich rare metal granite: the borehole PTP-1, the Podlesí stock, Krušné hory Mts., Czech Republic. Acta Univ. Carol., Geol. 42, 28–31.

Chlupáčová M., Mrázová Š. (2001): Anisotropy of magnetic susceptibility in granites of the Podlesí stock. In: Breiter K. (ed.) International Workshop Phosphorus- and Fluorine-rich fractionated granites, Podlesí. p. 9. Czech. Geol. Surv. Praha.

Duke E. F., Papike J. J., Laul J. C. (1992): Geochemistry of a boron-rich peraluminous granite pluton: the Calamity Peak layered granite-pegmatite complex, Black Hills, South Dakota. Canadian Mineralogist 30, 811–833.

Eisenreich M., Breiter K. (1993): Krupka, deposit of Sn-W-Mo ores in the eastern Krušné hory Mts. Věstník Čes. geol. Úst. 68, 15–22.

Fedkin A., Bezmen A., Seltmann R., Zaraisky G. (2002): Experimental simulation of a layered texture in the F-P-rich granite system. Bull. Czech. Geol. Surv., 77, 2, 113–125.

Förster H.-J. (2001): The radioactive accessory-mineral assemblage of the Podlesí granite-pegmatite system, western Krušné hory, Czech Republic: Implication to intrusion age and magmatic/hydrothermal fluid-rock interaction. In: Breiter K. (ed.) International Workshop Phosphorus- and Fluorine-rich fractionated granites, Podlesí. p. 9. Czech. Geol. Surv. Praha.

Frýda J., Breiter K. (1995): Alkali feldspars as a main phosphorus reservoirs in rare metal granites. three examples from the Bohemian Massif (Czech Republic). Terra Nova 7, 315–320.

Icenhower J., London D. (1996): Experimental partitioning of Rb, Cs, Sr, and Ba between alkali feldspars and peraluminous melt. Amer. Mineralogist 81, 719–734.

Jarchovský T. (1962): Entstehung der Feldspatsaume (Stockscheider) an den Kontakten von Granit- und Greisen-Stocken im Erzgebirge. Kristalinikum 1, 71–80.

Jarchovský T., Pavlů D. (1991): Albite-topaz microgranite from Horní Slavkov (Slavkovský les Mts.) NW Bohemia. Věst. Ústř. Úst. geol. 66, 13–22.

Kirkham R. V., Sinclair W. D. (1988): Comb quartz layers in felsic intrusions and their relationship to porphyry deposits. In: Taylor R.P. and

Strong D.F. (eds) Recent advances in the Geology of Granite-Related Mineral Deposits CIM Spec. vol. 31, 50–71.
Komárek (1968): Mineralogy and petrography of greisens from the Horní Blatná granite body. MS Czech Geological Survey Praha. (in Czech)
Kormilitsyn V. S., Manujlova M. M. (1957): Rhytmic banded quartz porphyry, Bugdai Mountain, southeast Transbaykal region. Zapiski Vsesoyuz. Mineral. Obshch. 86, 355–364. (in Russian)
Kostitsyn Ju. A., Breiter K. (2001): Rb-Sr isotopic dating of the Podlesí granites. In: Breiter K. (ed.) International Workshop Phosphorus- and Fluorine-rich fractionated granites, Podlesí. p. 22. Czech Geol. Surv. Praha.
Lhotský P., Breiter K., Bláha V., Hrochová H. (1988): Economic-geological investigations of Sn-mineralization near Podlesí in the western Krušné hory Mts. MS Czech Geological Survey Praha. (in Czech)
London D. (1992): The application of experimental petrology to the genesis and crystallization of granitic pegmatites. Canadian Mineralogist 30, 499–540.
London D. (1995): Geochemical features of peraluminous granites, pegmatites, and rhyolites as sources of lithophile metal deposits. In: Thompson J. F. H. (ed.) Magmas, fluids, and ore deposits. MAC Short Course 23, 175–202.
London D. (1996): Granitic pegmatites. Trans. Royal Soc. Edinburgh, Earth Sci. 87, 305–319.
London D. (1999): Melt boundary-layers and the growth of pegmatitic textures. Canadian Mineralogist 37, 826–827.
London D., Morgan G. B.VI, Babb H. A., Loomis J. L. (1993): Behaviour and effect of phosphorus in system Na_2O-K_2O-Al_2O_3-SiO_2-P_2O_5-H_2O at 200 MPa (H_2O). Contrib. Mineral. Petrol. 113, 175–202.
London D., Morgan G. B. VI, Hervig R. L. (1989): Vapor-undersaturated experiments with Macusani glass + H_2O at 200 MPA, and the internal differentiation of granitic pegmatites. Contrib. Mineral. Petrol. 102, 1–17.
London D., Morgan G. B. VI, Wolf M. B. (2001): Amblygonite-montebrasite solid solutions as monitors of fluorine in evolved granitic and pegmatitic melts. Amer. Mineralogist 86, 225–233.
Lowenstern J. B., Sinclair W. D. (1996): Exsolved magmatic fluid and its role in the formation of comb-layered quartz at the Cretaceous Logtung W-Mo deposit, Yukon Territory, Canada. Trans. Royal Soc. Edinburgh, Earth Sci. 87, 291–303.
Manning D. A. C. (1981): The effect of fluorine on liquidus phase relationships in the system Qz-Ab-Or with excess water at 1 kbar. Contrib. Mineral. Petrol. 76, 206–215.
McBirney A. R., Noyes R. M. (1979): Crystallization and layering of the Skaergaard intrusion. J. Petrology 20, 487–554.
Morgan G. B. VI, London D. (1999): Crystallization of the Little Three layered pegmatite-aplite dike, Ramona District, California. Contrib. Mineral. Petrol. 136, 310–330.
Müller A., Kronz A., Breiter K. (2001): Trace elements and growth patterns in quartz: a fingerprint of the evolution of the subvolcanic Podlesí Granite System (Krušné hory, Czech Republic). In: Breiter K. (ed.) International Workshop Phosphorus- and Fluorine-rich fractionated granites, Podlesí. 25–27. Czech Geol. Surv. Praha.
Müller A., Kronz A., Breiter K. (2002): Trace elements and growth patterns in quartz: a fingerprint of the evolution of the subvolcanic Podlesí Granite System (Krušné hory Mts., Czech Republic). Bull. Czech Geol. Surv. 77, 2, 135–145.
Mysen B.O. (1987): Magmatic silicate melts: relations between bulk composition, structure and properties. In: Mysen B.O. (ed) Magmatic processes. Physicochemical principles. Geochem. Soc. Spec. Publication 1, 375–400. New York.
Oelsner O. W. (1952): Die pegmatitisch-pneumatolitischen Lagerstätten des Erzgebirges mit Ausnahme der Kontaktlagerstätten. Freib. Forsch.-H., C4, 1–80.
Povilaytis M. M. (1961): About rhythmical zoning of some granitoids. Izvestiya Akad. Nauk SSSR, Ser. Geol. 2, 35–49. (in Russian)
Schalch F., Müller H., Gäbert C. (1900): Geologische Spezialkarte des Königreiches Sachsen 1:25 000, section No. 146 Johanngeorgenstadt. 2. Auflage. Dresden.
Schust F., Wasternack J. (1972): Über das Auftreten von Schlotformigen Brekzienkörpern bei Gottesberg und Mühlleithen im Granitmassiv von Eibenstock, Erzgebirge. Z. angew. Geol. 18, 400–410.
Schwarz M. O. (1991): Geochemical criteria for distinguishing magmatic and metasomatic albite-enrichment in granitoids. In: Pagel and Leroy (eds) Source, transport and deposition of Metals. 811–814. Balkema.
Seltmann R., Schilka W. (1991): Metallogenic aspects of breccia-related tin granites in the eastern Erzgebirge. Z. geol. Wiss. 19, 485–490.
Shannon J. R., Walker B. M., Carten R. B., Geraghty E. P. (1982): Unidirectional solidification textures and their significance in determining relative ages of intrusions at the Hederson Mine, Colorado. Geology 10, 293–297.
Skála R., Frýda J., Breiter K. (1998): Li-F micas from the granite stock at Podlesí, Czech Republic. Acta Univ. Carol., Geol. 42, 129–133.
Stephenson P. J. (1990): Layering in felsic granites in the main East pluton, Hinchinbrook Island, North Queensland, Australia. Geological Journal, 25, 325–336.
Táborská Š., Breiter K. (1998): Magnetic anisotropy of an extremely fractionated granite: the Podlesí stock, Krušné hory Mts. Acta Univ. Carol., Geol. 42,147–149.
Thomas R., Webster J. D., Heinrich W. (2000): Melt inclusions in pegmatite quartz: complete miscibility between silicate melts and hydrous fluids at low pressure. Contrib. Mineral. Petrol. 139, 394–401.
Tindle A. G., Webb P. C. (1990): Estimation of lithium contents in trioctahedral micas using microprobe data: application to micas from granitic rocks. Eur. J. Mineral. 2, 595–610.
Webber K. L., Falster A. U., Simmons W. B., Foord E. E. (1997): The role of diffusion-controlled oscillatory nucleation in the formation of line rock in pegmatite-aplite dikes. J. Petrology 38, 1777–1791.
Webster J. D., Thomas R., Rhede D., Förster H. J., Seltmann R. (1997): Melt inclusions in quartz from evolved peraluminous pegmatite: geochemical evidence for strong tin enrichment in fluorine- and phosphorus-rich residual liquids. Geochim. Cosmochim. Acta 61, 2589–2604.
Weis Z., Rieder M., Smrčok L., Petříček V., Bailey S. W. (1993): Refinement of the crystal structures of two “protolithionites”. Eur. J. Mineralogy, 5, 493–502.
Wolf M. B., London D. (1997): Boron in granitic magmas: stability of tourmaline in equilibrium with biotite and cordierite. Contrib. Mineral. Petrol. 130, 12–30.
Zaraisky G. P., Seltmann R., Shatov V. V., Aksyuk A. M., Shapovalov Yu. B., Chevychelov V. Yu. (1997): Petrography and geochemistry of Li-F granites and pegmatite-aplite banded rocks from the Orlovka and Etyka tantalum deposits in Eastern Transbaikalia, Russia. In: Papunen (ed.) Mineral deposits. 695–698. Rotterdam.
Žák K., Pudilová M., Breiter K. (2001): Oxygen isotope study of the highly fractionated Podlesí granite system – Preliminary data. In: Breiter K. (ed.) International Workshop Phosphorus- and Fluorine-rich fractionated granites, Podlesí. 34–35. Czech Geol. Surv. Praha.

Appendix

Methods

Electron microprobe analysis of minerals in the Czech Geological Survey: Minerals were analysed using a CAMSCAN 4-90DV electron microscope equipped with LINK eXL and Microspec WDX-3PC X-ray analysers. An accelerating voltage of 10 kV, a beam current of 3nA and a counting time of 100 s were used for the EDX analyses of Si, Ti, Al, Fe, Mn, Mg, Ca, Na, K, P, Nb, Ta and W, and the detection limits are 0.1 wt%. The WDX system was used for the analyses of F (PET, 10 kV, 100 nA) and Rb (TAP, 20 kV, 50 nA). The detection limits for F and Rb are 0.01 wt%.

C a t h o d o l u m i n i s c e n c e : The samples were analysed using cathodoluminescence equipment with hot cathode HC2-LM, Simon Neuser, Bochum, accelerating voltage 14 kV, beam density 10 m A/mm^2 in laboratory of Masaryk University Brno with help of J. Leichmann and in laboratory of University Göttingen with help of A. Müller.

W h o l e - r o c k c h e m i c a l a n a l y s e s : Major elements were analysed using standard methods of wet chemistry in the Laboratory of the CGS Praha, Pb, Rb, Sn, Zn, Zr by XRF in the Laboratory of the CGS Praha, other trace elements were analysed using ICP-MS in ACME Laboratory Vancouver.

Handling editor: Jan Pašava